Global Change Biology (2008) **14**, 2636–2660, doi: 10.1111/j.1365-2486.2008.01674.x

Simple three-pool model accurately describes patterns of long-term litter decomposition in diverse climates

E. CAROL ADAIR*†, WILLIAM J. PARTON‡§, STEVEN J. DEL GROSSO‡§, WHENDEE L. SILVER¶, MARK E. HARMON‖, SONIA A. HALL**, INGRID C. BURKE§†† and STEPHEN C. HART‡‡§§

*Department of Ecology, Evolution, and Behavior, University of Minnesota, Saint Paul, 1987 Upper Buford Circle, MN 55108, USA, †Department of Forest Resources, University of Minnesota, Saint Paul, MN 55108, USA, ‡Natural Resource Ecology Laboratory, Colorado State University, Fort Collins, CO 80523, USA, §Graduate Degree Program in Ecology, Colorado State University, Fort Collins, CO 80523, USA, ¶Ecosystem Sciences Division, Department of Environmental Science, Policy, and Management, University of California, Berkeley, CA, USA, ‖Department of Forest Sciences, Oregon State University, Corvallis, OR 97331, USA, **The Nature Conservancy, North Central Washington Field Office, Wenatchee, WA 98801, USA, ††Department of Forest, Rangeland, and Watershed Stewardship, Colorado State University, Fort Collins, CO 80523, USA, ‡‡School of Forestry, Northern Arizona University, PO Box 15018, Flagstaff, AZ 86011-5018, USA, §§Merriam-Powell Center for Environmental Research, Northern Arizona University, PO Box 15018, Flagstaff, AZ 86011-5018, USA*

Abstract

As atmospheric CO_2 increases, ecosystem carbon sequestration will largely depend on how global changes in climate will alter the balance between net primary production and decomposition. The response of primary production to climatic change has been examined using well-validated mechanistic models, but the same is not true for decomposition, a primary source of atmospheric CO_2. We used the Long-term Intersite Decomposition Experiment Team (LIDET) dataset and model-selection techniques to choose and parameterize a model that describes global patterns of litter decomposition. Mass loss was best represented by a three-pool negative exponential model, with a rapidly decomposing labile pool, an intermediate pool representing cellulose, and a recalcitrant pool. The initial litter lignin/nitrogen ratio defined the size of labile and intermediate pools. Lignin content determined the size of the recalcitrant pool. The decomposition rate of all pools was modified by climate, but the intermediate pool's decomposition rate was also controlled by relative amounts of litter cellulose and lignin (indicative of lignin-encrusted cellulose). The effect of climate on decomposition was best represented by a composite variable that multiplied a water-stress function by the Lloyd and Taylor variable Q_{10} temperature function. Although our model explained nearly 70% of the variation in LIDET data, we observed systematic deviations from model predictions. Below- and aboveground material decomposed at notably different rates, depending on the decomposition stage. Decomposition in certain ecosystem-specific environmental conditions was not well represented by our model; this included roots in very wet and cold soils, and aboveground litter in N-rich and arid sites. Despite these limitations, our model may still be extremely useful for global modeling efforts, because it accurately ($R^2 = 0.6804$) described general patterns of long-term global decomposition for a wide array of litter types, using relatively minimal climatic and litter quality data.

Keywords: cellulose, climate decomposition index, fine root, leaf, LIDET, lignin, litter quality, Q_{10} function

Received 23 February 2007 and accepted 4 May 2007

Correspondence: E. Carol Adair, Department of Ecology, Evolution, and Behaviour, University of Minnesota, 1987 Upper Buford Circle, MN 55108, USA, fax + 1 612 624 6777, e-mail: adair016@umn.edu

Introduction

Terrestrial ecosystems may serve either as a negative or as a positive feedback mechanism for future climate change (Burke *et al*., 2003; Weltzin *et al*., 2003). The future role of

these ecosystems will depend on how global changes alter the balance between carbon (C) inputs from net primary production and C losses from plant detritus and soil, which consist primarily of losses through decomposition. Annually, the decomposition of plant detritus (i.e. litter) and soil organic matter adds over 10 times more CO_2 to the atmosphere than fossil fuel and industrial sources (Schlesinger, 1997; Prentice *et al*., 2001). This, in combination with the precipitous rise in atmospheric CO_2 since the industrial revolution, suggests that even small changes in decomposition rates could have large impacts on atmospheric concentrations of CO_2.

Despite the potentially critical role of decomposition in the global C balance, our understanding of decomposition and the soil system remains rudimentary, particularly compared with our current understanding of C inputs through primary production (Ågren *et al*., 1991; Potter *et al*., 1993; McGuire *et al*., 1995, 1997). Although most research agrees that temperature, precipitation, and litter chemistry (C chemistry and nutrient content) strongly control rates of litter decomposition (Meentemeyer, 1978; Berg & Ågren, 1984; Aber *et al*., 1990; Hobbie, 2005), how these factors independently or interactively influence decomposition across large spatial and temporal scales remains unclear. Decomposition studies are most often local or regional in scale and use a low diversity of litter types and chemistries (Gholz *et al*., 2000). Extrapolating to global scales or nonrepresented litters and ecosystems is therefore problematic. Similarly, because most studies are conducted for less than 5 years, there are few data available to define how litter chemistry and climate control long-term or late-phase decomposition (Trofymow *et al*., 2002).

At the same time that efforts to model primary production have converged, the diversity of approaches used to describe and predict decomposition has remained high, perhaps due to the use of local, short-term datasets containing limited litter types to define and build decomposition models, and the relative lack of sophisticated decomposition model comparisons (vs. photosynthesis model comparisons; Pan *et al*., 1998). Most (if not all) decomposition models use temperature and moisture functions to control rates of decomposition, but the functional forms of the relationships vary widely (Burke *et al*., 2003; Del Grosso *et al*., 2005). The way litter quality is assumed to control decomposition rates varies even more dramatically – ranging from models that include very minimal litter quality effects (e.g. BIOME BGC) to those that divide litter into three or more pools based on various aspects of litter chemistry (e.g. CENTURY and G'DAY). Perhaps unsurprisingly, model reviews and comparisons have revealed discrepancies that suggest that a deeper understanding of global controls on decomposition is needed (Moorhead *et al*., 1999; Luckai & Larocque, 2002; Burke *et al*., 2003; Kirschbaum, 2006).

In contrast to the majority of decomposition datasets, the Long-term Intersite Decomposition Experiment Team (LIDET) dataset is 10-year, spatially extensive, and contains a wide range of litter quality substrates. The extensive nature of this dataset allowed us to compare and test many different hypotheses (i.e. models) about how climate and litter chemistry interact to control litter decomposition at large scales.

Hypotheses

We use the entire LIDET dataset to test five core *a priori* hypotheses about large-scale patterns of decomposition against alternative hypotheses formulated from shorter-term and smaller-scale decomposition datasets (e.g. Meentemeyer, 1978; Parton *et al*., 1994; Hobbie, 2005). Our objective was to test these hypotheses in a hierarchical manner, so that the end result would be the selection and parameterization of a relatively simple semimechanistic model that predicts long-term patterns of decomposition based only on climate and initial litter quality characteristics.

Hypothesis 1 (H1): Three initial litter pools representing different C qualities are needed to accurately describe patterns in long-term litter mass loss

Most models assume that litter quality affects the rate of litter decomposition and choose to represent this assumption by dividing litter into different 'pools' determined by the chemical composition of the litter. This division is based on research indicating that labile or soluble C compounds such as sugars and amino acids decompose most rapidly, followed by nonlignified cellulose and hemicellulose, and then lignified cellulose and lignin (Minderman, 1968; Berg *et al*., 1982; Berg & Ågren, 1984; Aber *et al*., 1990). This approach is employed in many ecosystem models, which divide litter into two or three pools that represent fast and slow decomposition based on initial C chemistry (Parton *et al*., 1987; Aber *et al*., 1990; Moorhead *et al*., 1999; Corbeels *et al*., 2005). We hypothesized that patterns of long-term decomposition would be best described by a three-pool decomposition model, with the initial mass of each pool determined by initial litter C chemistry, and the decomposition rate of each pool modified by climate.

Hypothesis 2 (H2): Increasing initial litter content of lignin relative to cellulose decreases the decomposition rate of litter cellulose

After the early period of litter decomposition, free or nonprotected cellulose is decomposed and the remaining cellulose is physically shielded by lignin encrustations (i.e. the lignin–carbohydrate matrix of plant cell walls; Chesson, 1997). The remaining cellulose cannot be decomposed independently of lignin, and litter decomposition becomes limited by the decomposition rate of lignin (Berg *et al*., 1982, 1984; McClaugherty & Berg, 1987; Aber *et al*., 1990). Given that a certain proportion of cellulose is protected by lignin (Melillo *et al*., 1989; Corbeels *et al*., 2005), we hypothesized that the decomposition rate of the nonsoluble fraction of litter would be modified by the relative amounts of lignin and cellulose.

Hypothesis 3 (H3): The size of the labile litter pool is inversely correlated to the initial lignin/nitrogen (L/N) ratio of the litter

Because initial decomposition rates increase with litter N concentrations (Berg *et al*., 1982; Hobbie, 2005), many models determine the size of initial litter pools using an N-related index. For example, in CENTURY, low L/N ratios increase the size of the labile litter pool, resulting in higher initial rates of decomposition (Parton *et al*., 1987, 1994). We hypothesized that the initial size of the fast pool in our best model from H2 would increase with initial N concentration and decrease with recalcitrant C concentration (i.e. lignin).

Hypothesis 4 (H4): A composite climate variable that incorporates the effects of temperature and soil moisture better represents the effect of climate on decomposition than variables that do not

Decomposition generally increases with temperature and moisture. However, at the extremes, and for some combinations of temperature and moisture, the relationships may be more complex. For instance, high temperatures can lead to moisture limitations if precipitation is not sufficient. This interaction is best represented by a composite climatic index that combines moisture and temperature effects. Gholz *et al*. (2000) found composite variables [e.g. actual evapotranspiration (AET) and CENTURY's synthetic variable DEFAC] to be more robust predictors of climatic effects on early phase decomposition than mean annual temperature (MAT) or mean annual precipitation (MAP) alone. Our goal was to compare the ability of MAP and MAT with the ability of two composite synthetic climate variables, AET and a climatic decomposition index (CDI, a synthetic variable that allows temperature and water stress to interact) to predict long-term litter decomposition at global scales.

Hypothesis 5 (H5): At a global scale, the effects of temperature on decomposition are best represented by a variable Q_{10} function because the temperature sensitivity of decomposition is greater during periods of lower temperatures

Q_{10} (Quotient 10) functions describe how processes such as decomposition or soil respiration change over 10°C intervals. Global decomposition models often use constant Q_{10} functions (e.g. Raich & Potter, 1995), but Del Grosso *et al*. (2005) found that CDIs with variable Q_{10} temperature functions were better able to describe the effect of temperature on soil respiration at large spatial scales. Most soil respiration data suggest that temperature sensitivity of decomposition is greatest at low temperatures, with low Q_{10} values at high temperatures and high Q_{10} values at low temperatures (Lloyd & Taylor, 1994; Kirschbaum, 1995; Del Grosso *et al*., 2005). Our goal was to compare the ability of a CDI with a constant Q_{10} temperature function with five CDIs that each incorporates a commonly used variable Q_{10} function to predict the effect of global variation in climate on litter mass loss.

Our objectives for this paper are (1) to test each of the hypotheses above in a formal structure that allows us to select a single, overall, best model and (2) to interpret systematic deviations from the model to improve our understanding of the controls on decomposition. Our prediction is that such systematic deviations will be related to differences among ecosystems (e.g. nutrient availability, extreme climate) or litter type and location (aboveground vs. belowground).

Materials and methods

LIDET study and design

The temporally and spatially extensive LIDET dataset (LIDET, 1995) allowed us to simultaneously contrast a large number of alternative hypotheses about long-term, global trends in decomposition. LIDET was initiated in 1990 to study the effects of substrate quality and macroclimate on decomposition of fine litter over a 10 year period (LIDET, 1995; Gholz *et al*., 2000). The project was a reciprocal litterbag study involving the transplanting of leaf and root litter from 26 species across 27 sites in North and Central America (Tables 1 and 2) that reflected a wide variety of natural ecosystems and climates (Gholz *et al*., 2000).

Nine 'standard' litters covering a wide range of L/N ratios were incubated at each site for 10 years beginning in 1990. Three species of fine roots and six species of leaf litter (Table 2), were confined in 20 cm^2 litterbags, with four replicate bags for each species, site, and time. Each site also had a 'wildcard' litter that appeared at only one

Table 1 Climatic characteristics and ecosystem types of the 27 LIDET (Long-term Intersite Decomposition Experiment Team) sites

Site	Site code	Latitude (°)	Longitude (°)	Elevation (m)	MAP (mm)	MAT (°C)	AET (mm)	PET (mm)	CDI_{LT}	DI (mm)	Ecosystem type
H. J. Andrews Experimental Forest	AND	44.23	122.18	500	2310	9.17	764	982	0.371	−362	Temperate conifer
Arctic Lakes	ARC	68.63	149.57	760	327	−8.87	284	423	0.129	−137	Alpine/ grassland
Barro Colorado Island	BCI	9.17	79.85	30	2692	27.17	1368	1517	1.713	842	Wet tropical
Bonanza Creek Experimental Forest	BNZ	64.75	148.00	300	403	−1.76	360	576	0.156	−266	Boreal conifer
Blodgett Research Forest	BSF	38.87	105.65	1300	1245	11.30	753	1097	0.259	−598	Temperate conifer
Cedar Creek Natural History Area	CDR	45.40	93.20	230	823	7.06	733	1026	0.483	−86	Humid grassland
Central Plains Experimental Range – Short Grass Steppe	CPR	40.82	104.77	1650	440	8.60	430	1202	0.243	−522	Dry grassland
Coweeta Hydrological Laboratory	CWT	35.00	83.50	700	1906	13.34	1173	1353	0.701	−163	Temperate deciduous
Guanica State Forest	GSF	17.95	65.87	80	508	26.38	503	1422	0.832	−408	Dry tropical
Hubbard Brook Experimental Forest	HBR	43.93	71.75	300	1396	5.55	713	818	0.463	15	Temperate deciduous
Harvard Forest	HFR	42.53	72.17	335	1152	7.49	851	1041	0.420	−336	Temperate deciduous
Jornada Experimental Range	JRN	32.50	106.75	1410	298	17.15	292	1666	0.216	−750	Shrubland
Juneau	JUN	58.00	134.00	100	2878	4.28	495	544	0.323	642	Boreal conifer
Kellogg Biological Station	KBS	42.40	85.40	288	811	8.84	708	1007	0.467	−314	Agriculture
Konza Prairie Research Natural Area	KNZ	39.08	96.58	366	791	12.57	747	1250	0.550	−328	Humid grassland
LaSelva Biological Station	LBS	10.00	83.00		4100	26.19	1699	1773	1.870	1354	Wet tropical
Luquillo Experimental Forest	LUQ	18.32	65.82	350	3363	23.48	1234	1260	1.609	837	Wet tropical

Continued

Table 1 *Continued*

Site	Site code	Latitude (°)	Longitude (°)	Elevation (m)	MAP (mm)	MAT (°C)	AET (mm)	PET (mm)	CDI_{LT}	DI (mm)	Ecosystem type
Loch Vale Watershed	LVW	40.28	105.65	3160	1096	1.71	851	1083	0.229	−174	Alpine/forest
Monte Verde	MTV	10.30	84.80	1550	2685	17.68	1084	1166	0.997	953	Wet tropical
North Inlet (Hobcaw Barony)	NIN	33.50	79.22	2	1491	18.20	1207	1456	0.983	−124	Saltmarsh/ wetland
Northern Lakes/ North Temperate Lakes	NLK	46.00	89.67	500	677	4.14	649	884	0.341	−223	Temperate conifer
Niwot Ridge/Green Lakes Valley	NWT	40.05	105.60	3650	1250	−3.21	647	756	0.145	−51	Alpine grassland
Olympic National Park	OLY	47.83	123.88	150	1531	10.73	794	1044	0.370	−406	Temperate conifer
Sevilleta National Wildlife Refuge	SEV	34.33	106.67	1572	255	13.17	252	1602	0.136	−848	Shrubland
Santa Margarita Ecological Reserve	SMR	33.50	117.75	500	240	14.64	236	1860	0.150	−931	Shrubland
University of Florida	UFL	29.75	82.50	35	1238	20.72	1166	1621	1.041	−247	Temperate conifer
Virginia Coast Reserve	VCR	37.50	75.67	0	1138	15.03	993	1215	0.761	−265	Saltmarsh/ wetland

All climatic variables were calculated for the 10 years of available data closest to the LIDET study period (1990–1999). CDI_{LT} is the Lloyd & Taylor (1994) climate decomposition index (CDI) and DI is a drought index, which indicates growing season water deficit (May–September precipitation – PET; Liski *et al.*, 2003).
MAP, mean annual precipitation; MAT, mean annual temperature; AET, actual evapotranspiration; PET, potential evapotranspiration.

Table 2 Initial values of litter quality indices for species in the LIDET (Long-term Intersite Decomposition Experiment Team) experiment

Species	Litter type	Abbreviation	WSE (%)	Cellulose (%)	Lignin (%)	Tannins (%)	C (%)	N (%)	L/cell	L/N	C/N	L_s
Leaf litter												
Yellow Birch (*Betula lutea*)	Broadleaf	BELU	18.52	45.78	26.62	2.60	49.88	1.60	0.58	16.64	31.19	0.368
Buckthorn (*Ceanothus greggii*)	Shrub	CEGR	49.11	26.87	12.37	8.09	52.58	1.33	0.46	9.32	39.71	0.315
*Drypetes (*Drypetes glauca*)	Broadleaf	DRGL	40.23	39.82	10.91	8.02	47.79	1.97	0.27	5.53	24.25	0.215
Creosote Bush (*Larrea tridentata*)	Shrub	LATR	31.54	40.46	7.95	5.92	50.85	2.14	0.20	3.72	23.81	0.164
Black Locust (*Robinia pseudoacacia*)	Broadleaf	ROPS	33.77	40.45	17.66	5.32	50.19	2.45	0.44	7.21	20.49	0.304
*Slash Pine (*Pinus elliottii*)	Conifer	PIEL	19.60	41.34	21.42	4.55	54.26	0.36	0.52	59.49	163.83	0.341
Pacific Rhododendron (*Rhododendron macrophyllum*)	Broadleaf	RHMA	36.27	36.90	16.95	6.25	50.80	0.42	0.46	40.60	126.28	0.315
*Wheat (*Triticum aestivum*)	Gramminoid	TRAE	6.72	73.15	16.21	2.93	47.32	0.38	0.22	42.94	133.32	0.181
Subalpine Fir (*Abies lasiocarpa*)	Conifer	ABLA	31.96	30.65	17.96	6.20	53.97	0.71	0.59	25.29	76.07	0.369
Beach Grass (*Ammophila breviligulata*)	Gramminoid	AMBR	21.57	56.90	14.40	4.69	48.63	0.67	0.25	21.57	73.47	0.202
Big Bluestem (*Andropogon gerardii*)	Gramminoid	ANGE	14.74	59.37	18.68	1.80	44.55	0.62	0.31	30.25	73.11	0.239
*Red Pine (*Pinus resinosa*)	Conifer	PIRE	20.60	44.58	19.18	7.41	53.41	0.59	0.43	32.64	92.72	0.301
Eastern White Pine (*Pinus strobus*)	Conifer	PIST	20.17	39.68	20.59	4.82	52.84	0.62	0.52	33.08	85.86	0.342
*Western Redcedar (*Thuja plicata*)	Conifer	THPL	22.31	35.92	26.67	2.96	51.13	0.62	0.74	42.85	83.12	0.426
*Sugar Maple (*Acer saccharum*)	Broadleaf	ACSA	47.68	27.33	15.87	7.73	49.77	0.81	0.58	19.65	61.83	0.367
Black Grama (*Bouteloua eriopoda*)	Gramminoid	BOER	13.19	64.33	15.53	1.20	44.90	0.86	0.24	18.01	52.90	0.194
Blue Grama (*Bouteloua gracilis*)	Gramminoid	BOGR	13.84	68.58	7.96	1.90	42.96	0.96	0.12	8.29	44.96	0.104
Pacific Dogwood (*Cornus nuttalii*)	Broadleaf	CONU	51.74	37.01	0.76	9.35	44.13	0.81	0.02	0.94	55.81	0.020
Beech (*Fagus grandifolia*)	Broadleaf	FAGR	16.25	49.11	26.03	5.34	49.41	0.85	0.53	30.62	58.40	0.346
Kobresia (*Kobresia myosuroides*)	Gramminoid	KOMY	22.73	61.56	9.25	2.43	46.26	1.07	0.15	8.67	43.88	0.131
Tulip Poplar (*Liriodendron tulipifera*)	Broadleaf	LITU	43.62	31.27	8.70	5.19	46.36	0.72	0.28	12.08	65.06	0.218
Aspen (*Populus tremuloides*)	Broadleaf	POTR	28.43	40.77	18.76	4.58	49.21	0.74	0.46	25.52	67.24	0.315
Douglas-Fir (*Pseudotsuga menzesii*)	Conifer	PSME	22.02	37.27	27.35	1.53	48.75	0.82	0.73	33.36	60.27	0.423
*Chestnut Oak (*Quercus prinus*)	Broadleaf	QUPR	27.22	39.38	23.51	6.88	51.48	1.03	0.60	22.90	50.55	0.374
Spartina (*Spartina alterniflora*)	Gramminoid	SPAL	26.75	58.77	7.12	4.14	42.72	0.71	0.12	10.02	62.57	0.108
Roots												
*Big Bluestem (*Andropogon gerardii*)	Gramminoid	ANGE	13.62	67.06	10.54	1.08	37.01	0.63	0.16	16.72	59.42	0.136
*Drypetes (*Drypetes glauca*)	Broadleaf	DRGL	19.91	52.15	16.13	2.43	48.24	0.76	0.31	21.22	64.56	0.236
*Slash Pine (*Pinus elliottii*)	Conifer	PIEL	19.65	35.94	34.90	3.28	49.39	0.82	0.97	42.65	61.49	0.493
*Red Pine (*Pinus resinosa*)	Conifer	PIRE	9.37	56.34	28.20	2.25	48.44	1.22	0.50	23.21	39.87	0.334

Asterisks (*) denote the litter types that are the 'standard' species sent to each site for each time. There are a total of 25 leaf litter species and four root litter species. WSE, water-soluble extractives; L, lignin; N, nitrogen; cell, cellulose; C, carbon; and $L_S = L/(L + \text{cell})$. Each site has six standard aboveground litter types and three standard belowground litter types; seven aboveground and four belowground litter types are marked as standard in the table because supplies of *P. elliottii* (PIEL) were less than expected, so some sites received *P. resinosa* (PIRE) instead (i.e. each site has either PIEL or PIRE as a standard leaf or root litter type).

site for all sample collections. Leaf litterbags were constructed from 1 mm nylon mesh on the top (to allow access by most soil fauna; Hobbie, 2005) and 55 μm Dacron cloth on the bottom (to prevent fragmentation losses but allow access by fungal hyphae, bacteria, nematodes, and protozoa; Swift *et al*., 1979). Root litterbags were constructed entirely of 55 μm cloth. Litterbags were filled with 10 g of leaves and 5–7 g of fine roots. Ten sets of 10 litterbags were placed at each site. Leaf litterbags were placed on the ground surface. Fine root bags were placed within the top 20 cm of mineral soil at a 45° angle.

Although the litterbag method has some limitations, including burial of surface bags by falling litter through time, microclimatic effects, and potential exclusion of soil fauna (Hutchinson *et al*., 1990; Virzo De Santo *et al*., 1993; Kurz-Besson *et al*., 2005), it remains the best available method for generating large decomposition datasets because it is easy to implement and thus replicate consistently among a large number of observers and sites (Kurz-Besson *et al*., 2005). A pilot study found essentially no effect of mesh size (1 vs. 5 mm) on leaf decomposition, but a caution remains regarding the effects of mesh size on root decomposition, as no similar study was conducted for belowground decomposition (Gholz *et al*., 2000).

Litterbags were collected approximately each year at all sites except the tropical sites, where samples were collected every 3–6 months due to higher decomposition rates. Initial litter chemistry and ash content were determined at Oregon State University (Table 2; Gholz *et al*., 2000). Gholz *et al*. (2000) and LIDET (1995) provide a detailed description of field and laboratory methods.

Climatic data and parameters

We used observed precipitation and temperature data from the experimental period (1990–1999, Table 1) to calculate climate variables. The monthly water budget in the CENTURY model (Parton *et al*., 1994) was used to calculate AET for each site given the monthly average maximum and minimum air temperature and precipitation. We calculated potential evapotranspiration (PET; Allen *et al*., 1998) using solar radiation (calculated from latitude and time of year), monthly average daily minimum and maximum air temperature, and relative humidity.

In addition to these standard climatic descriptors, we calculated CDIs. A CDI is a function that describes the effect of monthly variation in temperature and water on decomposition. The water function we used assumes that water controls decomposition primarily through water stress. Thus, extremely high levels of soil moisture (e.g. waterlogged soils) may not be well-represented by our CDIs. Annual CDIs are the mean value of monthly CDI_is, which are calculated as a function of mean monthly air temperature (T_i), monthly precipitation (PPT_i), and monthly PET_i of the ith month:

$$CDI_i = F_T(T_i) \times F_W(PPT_i, PET_i), \quad (1)$$

$$F_T(T_i) = 0.5766 \times \exp\left[308.56 \times \left(\frac{1}{56.02} - \frac{1}{(273 + T_i) - 227.13}\right)\right], \quad (2)$$

$$F_w(PPT_i, PET_i) = \frac{1.0}{1.0 + 30 \times \exp(-8.5 \times PPT_i/PET_i)}, \quad (3)$$

where $F_W(PPT_i, PET_i)$ and $F_T(T_i)$ are the monthly effects of water stress and temperature on decomposition.

We calculated different CDIs by varying the temperature function (Fig. 1, Appendix A). Our initial analyses used a CDI with Lloyd & Taylor's (1994) variable Q_{10} temperature function [CDI_{LT}; Eqn (2)]. We later compared CDI_{LT} to five additional CDIs with different temperature functions, including a constant Q_{10} exponential function (CDI_{exp}) and four variable Q_{10} functions, to determine which CDI best predicted the effect of climate on decomposition. The variable Q_{10} temperature functions were as follows: a positive linear function (CDI_{linear}), an arctangent function (CDI_{atan}; Del Grosso *et al*., 2005), the Kirschbaum function (CDI_K; Kirschbaum, 1995), and the function used by the CENTURY model ($CDI_{DEFAC;}$ Parton *et al*., 1989, 1994). The Kirschbaum (1995) as well as the Lloyd & Taylor (1994) functions were empirically derived. The Kirschbaum (1995) equation was based on laboratory soil respiration measurements, and the Lloyd & Taylor (1994) equation

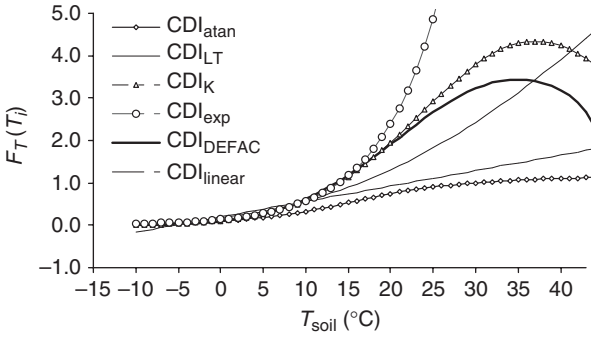

Fig. 1 Alternative temperature functions [$F_T(T_i)$ in Eqn (1); also see Appendix A] for the climate decomposition index (CDI). As in our analyses, the arctangent function is normalized to the value of the function at 30°C, while all other functions are non-normalized values.

was derived from field measurements of soil respiration. Gholz *et al*. (2000) and Moorhead *et al*. (1999) found CDI_{DEFAC} (referred to as DEFAC in these papers) to be well-correlated to litter decomposition rates. However, Del Grosso *et al*. (2005) found that CDI_{atan} predicted heterotrophic and autotrophic respiration rates better than other functions.

Data analysis

To explore each hypothesis, we developed a series of models based on the negative exponential decomposition equation (Olson, 1963). These models predicted mass loss at all sites over the 10-year experimental period based on the decomposition of one to three initial litter pools (M_1–M_3) over time. The size of each pool (percent of total initial litter mass) was determined by initial litter chemistry. These simple equations were modified by including a climate descriptor in the exponential term of each pool. The set of candidate models for each hypothesis was based on this simple framework (Appendix A).

We used Akaike's Information Criterion (AIC) modified for small sample sizes (AICc) to choose among the models in the candidate sets for each hypothesis. AIC combines the Kullback–Leibler (K–L) distance (the amount of information lost by using a model to approximate the truth) with maximum likelihood estimation by using likelihood to estimate the relative K–L distance between competing models. This method determines which model is closest to the unknown truth, which is represented by the data (Burnham & Anderson, 2002; Del Grosso *et al*., 2005). AIC is, therefore, used to rank a set of *a priori* models based on the support for each found in the data. The model with the lowest AICc value has the most support in the data and is closest to the unknown truth. The differences between the AICc value of the best model and the values of each model ranked below it (Δr = AICc of each model−AICc best model) provides information to evaluate whether models in the set are close competitors to the best model – the Δr of the best model is zero; models that are within 1–2 AICc points of the best model have substantial support in the data; relative to the best models in the set, models with $\Delta r > 7$ have essentially no support in the data (Burnham & Anderson, 2002). This methodology also provides information on model-selection uncertainty by calculating Akaike weights (w_r) for each model. Akaike weights are the probability that the best model would be selected again as best, given the same set of models and a new set of similar but independent data (Burnham & Anderson, 2002).

Our first hypothesis (H1) compared one-, two-, and three-pool models of decomposition to determine the number of pools that most accurately depicted long-term decomposition:

$$M_t = M_1 e^{-k_1 CDI_j t}, \quad (4)$$

$$M_t = M_1 e^{-k_1 CDI_j t} + M_2 e^{-k_2 CDI_j t}, \quad (5)$$

$$M_t = M_1 e^{-k_1 CDI_j t} + M_2 e^{-k_2 CDI_j t} + M_3 e^{-k_3 CDI_j t}, \quad (6)$$

where M_t is the percentage of mass remaining at time t (years), M_p the initial litter mass of each pool ($p = 1, 2$, or 3), $CDI_j = CDI_{LT}$ for each site (j), and k_p is the decomposition rate of each pool. Because our goal was to create a relatively simple decomposition model, we assumed that each litter pool was affected similarly by climate, and used the same CDI to modify the decomposition rate of each pool. Our initial analyses used only one CDI (CDI_{LT}) because H4 and H5 tested climate indices. We used measured initial C chemistry to define initial pool sizes, such that M_2 was percentage cellulose, M_3 was percentage lignin, and M_1 was the difference between 100% and the sum of M_2 and M_3 (thus, in the one-pool model, $M_1 = 100\%$, while in the two-pool model M_2 = percentage cellulose + percentage lignin and $M_1 = 100\% - M_2$). Our hypothesis that a three-pool model would be the best predictor of long-term decomposition would be supported if Eqn (6) was chosen using AICc model selection. While it may be expected that a three-pool model would have a higher probability of fitting the data (through overparameterization), using AICc helps us avoid this fate by including a penalty for increasing the number of parameters in a model and also by providing a quantitative assessment of the different model fits, allowing evaluation of how much models actually differ from each other.

Table 3 Litter quality indices (q) included in the main model selection run

	Litter quality index, q	
Index no.	Abbreviation	Explanation
1	Cell/L	Cellulose/lignin ratio
2	N/C	Nitrogen/carbon ratio
3	N/L	Nitrogen/lignin ratio
4	L_c	$L_c = \exp(-3 \times L_s)$, $L_s = L/(L + cell)$
5	$-b \times L_s$	$L_s = L/(L + cell)$, b is a data estimated parameter
6	1−L/cell	1−lignin/cellulose
7	(L + cell)/L	(cellulose + lignin)/lignin
8	None	

Each litter quality index (including no litter quality index) was used in a one-, two-, and three-pool model, for a total of 24 models for the model-selection analysis of hypothesis 2.

To test H2, we created a set of 'litter quality models' that again compared the one-, two-, and three-pool models, but now with different litter quality indices (q; Table 3) in either the first pool of single-pool models or the second pool of two- and three-pool models (24 models; Appendix A). As in H1, we confined our analysis to the use of one climate index, CDI_{LT} and initial pool sizes using measured C chemistry. If AICc chose a model that used the initial lignin and cellulose contents to control decomposition of M_2, our hypothesis that cellulose decomposition is influenced by the encrustation of cellulose by lignin would be supported.

To investigate the effect of initial litter N concentration on decomposition (H3), we used the best model from the litter quality model analysis (H2) to compare the effect of using the measured C fractions (as in H1 and H2) with using equations that were linear or exponential functions of initial litter L/N ratios to define initial pool sizes (Table 4). We refer to this set of models as the 'initial pool models.' Our decision to estimate initial litter pool sizes as a function of the L/N ratio was based on the assumption that litter N concentration most strongly impacts litter decomposition in the early phases of decomposition. This assumption has been successfully used to model ecosystem C cycling in the CENTURY model (Parton *et al*., 1994). Each of our equations used the initial L/N of each litter to change the size of M_1. Because M_3 is always equal to the measured lignin content, these equations also adjust the size of M_2. As the L/N ratio increases (typically because N decreases as lignin increases) the size of the M_1 pool decreases and M_2 increases. In this way, low L/N ratios increase the size of the M_1 pool, which decomposes most rapidly, thus increasing initial rates of decomposition.

In addition to the linear slope and intercept or exponential shape parameters, each model included a parameter that defined either the minimum size of the M_1 pool or maximum value of the L/N ratio, so that M_1 would always be greater than zero (Table 4). Our decision to include a minimum M_1 or maximum L/N parameter in each model was based on (1) the observation that labile C contents in litter (often measured as water soluble extractives, WSE) do not reach zero even if the litter has extremely high L/N ratios (minimum WSE ranges between 3% and 18% when L/N > 55; Trofymow, 1998; Hobbie & Gough, 2004; Hobbie, 2005) and (2) previous datasets that have found short term (1 year) decomposition rates and/or water soluble C contents to decrease with increasing L/N ratios until L/N = 50–60, after which each is relatively unaffected by further L/N ratio increases (Melillo & Aber, 1982; Harmon *et al*., 1990). We either used the LIDET dataset to estimate parameter values in these equations or defined parameter values *a priori* based on previous datasets (Table 4).

If the best litter quality model (H2) included a litter quality parameter that involved initial cellulose content (M_2), then two versions of that model were included:

Table 4 For hypothesis 3, the equations and maximum limits on either the size of $M_2 + M_3$ or lignin/nitrogen (L/N) ratio used to determine the most accurate method of determining initial pool sizes (in combination with the best model from hypothesis 2)

Method	M_1 litter quality index	Maximum $M_2 + M_3$ parameter source	Percentage of total litter				
			M_1	M_2	M_3	Maximum $M_2 + M_3$	Maximum L/N
Measureable chemistry	None		$100-(M_2+M_3)$	Percentage cellulose	Percentage lignin	na	na
Linear function of L/N		Estimated parameters	$100-(M_2+M_3)$	$[\beta_1+\beta_2 \times (L/N)]-M_3$	Percentage lignin	Estimated, 80%, 90%, 95%	Estimated, 50, 60
		Parton *et al*. (1994)	$100-(M_2+M_3)$	$[15+1.8 \times (L/N)]-M_3$	Percentage lignin	80%	
		CENTURY	$100-(M_2+M_3)$	$[15+1.3 \times (L/N)]-M_3$	Percentage lignin	80%	
Negative exponential fucntion of L/N		Estimated parameters	$\beta_0+\beta_1 \times \exp[-\beta_2 \times (L/N)]$	$100-(M_1+M_3)$	Percentage lignin	Estimated, 80%, 90%, 95% (β_0 = 20%, 10%, 5%)	Estimated, 50, 60 ($\beta_0 = 0$)

na, not applicable.

one that used the measured quantity of cellulose in the quality index and a second model that used the L/N function to estimate the size of the M_2 pool. Our hypothesis that L/N ratios affect early rates of decomposition would be supported if AICc chose a model that used one of our equations to determine initial pool size vs. the model that used measurable C chemistry.

Within H3, we compared the initial pool models to three models that allowed N content to influence rates of early decomposition by influencing the decomposition rate of M_1 (Appendix A). Because these models did not perform as well as the initial pool models (Appendix A), we focused on the initial pool models.

We used the best model from the initial pool models (H3) to compare MAT, MAP, AET, and the six alternative CDIs (H4 and H5). AICc was used to select the climate parameter that best predicted mass loss over time. Within this set of 'climate models,' we first compared noncomposite (MAP and MAT) with composite (AET and CDI_{exp}) climate indices (H4 and set 1 of the climate models), and then compared the six CDIs that used either constant or variable Q_{10} temperature functions (H5 and set 2 of the climate models). Our hypotheses would be supported if a composite CDI with a variable Q_{10} function was selected as the best model.

Finally, we investigated the dataset for systematic biases, defined as deviations from the best model predictions based on litter or ecosystem type. We expected any deviations to be based on ecosystem differences or litter type (above- and belowground). Ecosystem differences may be based on differences in nutrient availability, climate or abiotic extremes. We also considered the possibility that alternative processes, such as UV-enhanced decomposition may be influencing litter decomposition in some ecosystems (i.e. arid) but not others (e.g. moist tropical).

To investigate a litter type bias, we used AICc to determine if using the best model for all litter together was better than using the same model with data separated by litter type. In the second model, k_ps were estimated for leaf and root litter separately, but the parameters used to determine initial pool sizes (β_1 and β_2) were kept constant (as determined in H3). To evaluate site and ecosystem biases, we examined the correlation between the data and model predictions over time, both statistically and visually. In two cases (wetland and arctic sites), we used the same analysis as described above for separating by litter type. We also investigated biases revealed in temperate and tropical sites using the data for these sites alone. Because a portion of these investigations were *post hoc*, primarily the ecosystem biases, we emphasize that these relationships should be further investigated with independent datasets.

All tested models, associated AIC statistics, and model convergence information are listed in Appendix A. Appendix B presents the parameter estimate correlation matrices for the best models from H1 to H5.

Results

Hypotheses

H1: Three initial litter pools of differing carbon qualities best described patterns in long-term litter mass loss

Averaged across all sites, litter types, and species, litter mass loss was approximately 70% over the 10 year study period. The three-pool model selected by AICc as the best model captured over half of the variability in the LIDET dataset ($R^2 = 0.622$; Table 5). This model contained separate exponential decomposition rates (k_p) for the fast, slow, and recalcitrant C pools (Table 5). The k_ps for the three litter pools indicated fast

Table 5 For hypothesis 1, of the three models, a three-pool model provided the most accurate predictions of long-term decomposition at the LIDET (Long-term Intersite Decomposition Experiment Team) datasets than did one- or two-pool models

Model	N	R^2	P	AICc	Δr	w_r	k_1	k_2	k_3
$M_t = M_1 \times \exp(-k_1 \times \mathrm{CDI} \times t)$	2039	0.5326	<0.0001	11 873.3	908.5	5E-198	0.5278		
$M_t = M_1 \times \exp(-k_1 \times \mathrm{CDI} \times t)$ $+ M_2 \times \exp(-k_2 \times \mathrm{CDI} \times t)$	2039	0.5115	<0.0001	11 563.5	598.7	1E-130	2.1193	0.2803	
$M_t = M_1 \times \exp(-k_1 \times \mathrm{CDI} \times t)$ $+ M_2 \times \exp(-k_2 \times \mathrm{CDI} \times t)$ $+ M_3 \times \exp(-k_3 \times \mathrm{CDI} \times t)$	2039	0.6221	<0.0001	10 964.8	0.0	1	1.0669	0.7676	0

All models converged, and all parameters were constrained, $k_i \geq 0$. In the three-pool model, k_3 hit this lower bound and was set at zero for estimation of the remaining parameters. CDI (climatic decomposition index) = Lloyd & Taylor (1994) CDI.
AICc, Akaike's Information Criterion.

decomposition of the labile pool ($k_1 > 1$), slower decomposition ($k_2 \sim 0.8$) of the cellulose pool, and essentially no ($k_3 = 0$) decomposition of the lignin pool over the 10-year period (Table 5).

Of the one-, two-, and three-pool models examined under H1, only the three-pool model had a $\Delta r < 10$ ($\Delta r = 0$, $w_r = 1$), indicating that the LIDET dataset strongly supported the choice of the three-pool model. The one- and two-pool models had Δr values > 500 and w_r values < 0.00001, indicating that compared with the three-pool model, these models had essentially no support in the data and have virtually no chance of being chosen as the best model given the same model set and a similar set of independent data (Table 5).

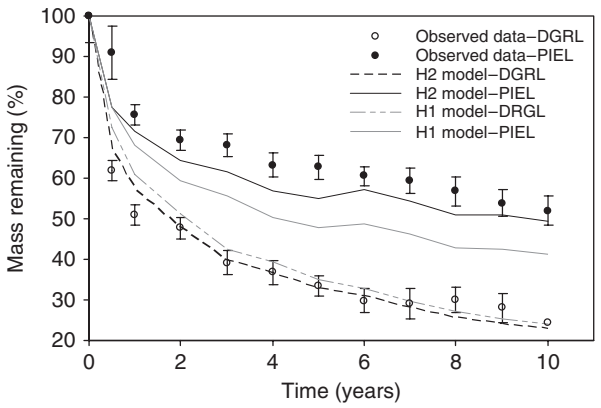

Fig. 2 Litter quality affects the rate of mass loss. Leaf litter of two species with different litter qualities is shown averaged across all sites: *Drypetes glauca* (DGRL; L/cell = 0.27 and L/N = 5.5) decays more rapidly than *Pinus elliottii* (PIEL; L/cell = 0.52 and L/N = 59.5). The predictions of best model from hypothesis 1 (H1 model) do not predict the decay rates of these two litter types as accurately as the best model from hypothesis 2 (H2 model). The H1 and H2 models are both three-pool models but litter quality modifies the decay rate of the M_2 litter pool in the H2 model. Error bars are ± 1 SE.

H2: Increasing initial litter content of lignin relative to cellulose decreased the decomposition rate of litter cellulose

Overall, litter quality had a dramatic impact on litter decomposition (Fig. 2). Including a litter quality index (q) that accounted for lignin protection or 'encrustation' of cellulose in the three-pool model significantly improved the prediction of mass loss over the simple three-pool model from H1, particularly after the second year of decomposition (Table 6, Fig. 2). The best litter quality model, as selected by AICc, allowed the lignin (L) fraction [L/(L + cellulose)] to modify the decomposition rate of the second, or slow pool (litter quality index #5, Table 3). This model had a $\Delta r = 0$ and $w_r = 0.918$, indicating very strong support in the data for this model (Table 6).

H3: Initial N concentration and C quality affected initial mass losses

Litters with low L/N ratios decomposed more rapidly than those with high ratios (Fig. 2). In combination with the best litter quality model (from H2), using the initial L/N ratio to estimate initial pool sizes resulted in better predictions of mass loss than using measured C pools to determine initial pool sizes (Table 7, Appendix A).

With very few exceptions, using the measured cellulose in the litter quality index of the best litter quality model from H2 [L_s = L/(L + cellulose)] was a better predictor of decomposition than using the L/N equation of each model to estimate the initial percent cellulose (M_2) for this parameter. For models with $\Delta r < 40$, the version of each model that used measured cellulose in L_s was always 4–9 AICc points lower (i.e. better) than the version that used estimated cellulose in L_s. For this reason, we focused on the models that used measured cellulose in L_s, with the knowledge that, in datasets

Table 6 The best three models from the set of litter-quality models (hypothesis 2, H2), compared with the best model from hypothesis 1 (H1; the three-pool model)

Model	N	R^2	P	AICc	Δr	w_r	k_1	k_2	k_3	b
$M_t = M_1 \times \exp(-k_1 \times \text{CDI} \times t) + M_2 \times \exp[-k_2 \times \text{CDI} \times \exp(-b \times L_s) \times t] + M_3 \times \exp(-k_3 \times \text{CDI} \times t)$	2039	0.6606	<0.0001	10708	0	0.918	1.893	1.5817	0.0343	4.271
$M_t = M_1 \times \exp(-k_1 \times \text{CDI} \times t) + M_2 \times \exp[-k_2 \times \text{CDI} \times ((\text{L} + \text{cell})/\text{L}) \times t] + M_3 \times \exp(-k_3 \times \text{CDI} \times t)$	2039	0.6583	<0.0001	10713	4.9	0.085	1.844	0.1314	0.0189	
$M_t = M_1 \times \exp(-k_1 \times \text{CDI} \times \text{t}) + M_2 \times \exp(-k_2 \times \text{CDI} \times \text{cell}/\text{L} \times t) + M_3 \times \exp(-k_3 \times \text{CDI} \times t)$	2039	0.6592	<0.0001	10719	11.0	0.004	1.987	0.1590	0.0554	
$M_t = M_1 \times \exp(-k_1 \times \text{CDI} \times t) + M_2 \times \exp(-k_2 \times \text{CDI} \times t) + M_3 \times \exp(-k_3 \times \text{CDI} \times t)$	2039	0.6221	<0.0001	10965	256.7	0	1.067	0.7676	0	

Including litter quality in the three-pool model from H1 clearly increases the predictive ability of the model. The best litter quality model includes a term that decreases the decomposition rate of M_2 with increasing lignin fraction, L_s [lignin/(cellulose + lignin)]. CDI (climatic decomposition index) = Lloyd & Taylor (1994) CDI. AICc, Akaike's Information Criterion.

Table 7 Best 10 models from hypothesis 3 (H3), the initial pool models, compared with the best model from hypothesis 2 (H2), the litter quality models

Model #	Rank	Pool estimation equation	Maximum definition	N	R^2	P	AICc	Δr	w_r	k_1	k_2	k_3	b	β_1	β_2	β_0 or maximum L/N	Size of $M_2 + M_3$ at maximum L/N or L/N = 100	#AICc points above model with L_{sest}
1	1	Linear	L/N = 60	2039	0.683	<0.0001	10 546.3	0	0.73	3.816	0.768	0.0234	1.249	52.434	0.817		101.5	9.6
2	2	Linear	L/N = estimated	2039	0.683	<0.0001	10 548.3	2.0	0.27	3.816	0.768	0.0234	1.249	52.434	0.817	72.55	111.7	9.6
3	5	Exponential	L/N = 60	2039	0.680	<0.0001	10 562.6	16.3	0.00	3.545	0.747	0.0270	1.324	57.167	0.030		90.6	6.7
4	6	Exponential	$M_2 + M_3$ = estimated	2039	0.680	<0.0001	10 564.6	18.3	0.00	3.546	0.747	0.0270	1.324	57.167	0.030	0	97.2*	6.7
5	7	Exponential	L/N = estimated	2039	0.680	<0.0001	10 564.6	18.3	0.00	3.546	0.747	0.0270	1.324	57.166	0.030	183.1	99.8	6.7
6	8	Exponential	$M_2 + M_3 = 95$	2039	0.680	<0.0001	10 567.4	21.1	0.00	3.339	0.737	0.0293	1.391	54.830	0.035		93.3*	5.7
7	10	Linear	L/N = 50	2039	0.679	<0.0001	10 570.4	24.1	0.00	4.124	0.783	0.0211	1.224	54.444	0.798		94.3	4.4
8	14	Exponential	$M_2 + M_3 = 90$	2039	0.678	<0.0001	10 574.3	28.0	0.00	3.059	0.723	0.0328	1.501	53.395	0.039		89.0*	4.4
9	15	Exponential	L/N = 50	2039	0.678	<0.0001	10 574.8	28.5	0.00	3.857	0.764	0.0232	1.252	55.484	0.032		88.8	3.5
10	19	Linear	L/N = 40	2039	0.677	<0.0001	10 585.9	39.6	0.00	4.468	0.794	0.0186	1.182	55.027	0.853		89.2	1.5
	32	Measured	na	2039	0.661	<0.0001	10 708.0	161.7	5.5E-36	1.893	1.582	0.0343	4.271				NA	NA

The H2 models used measured C quality to determine initial pool sizes while the H3 models used a function of the initial lignin/N (L/N) ratio of each litter type to determine initial pool sizes. Because the best two models did not provide realistic estimates of $M_2 + M_3$ (>100%), we chose model #3 as the best model for all further analyses. Asterisks (*) denote models that did not have a defined maximum. The final column in the table '# AICc points above model with est. L_s' is the number of AICc points between the model that used the measured percentage cellulose in the quality modifier (L_s) and the model that used the pool estimation equation to estimate the percentage cellulose in L_s (L_{sest}). In the 10 best models, the model using the measured cellulose in L_s had a lower Δr than the same model using estimated percentage cellulose. na, not applicable; AICc, Akaike's Information Criterion.

where measured cellulose is unavailable, estimating cellulose as a function of L/N may be a reasonable approximation.

Estimating a maximum limit on the size of $M_2 + M_3$ produced unrealistic results for the LIDET dataset. The two best models had maximum L/N ratios, but the size of $M_2 + M_3$ was >100% at these maxima (Table 7). This could be because our dataset included only one litter type with a L/N ratio >50 (Table 2). Litter with initial L/N ratios >70 have been used in several decomposition studies, and it is in these datasets that the asymptotic relationship between L/N and fast decomposition rates or labile C is most apparent (Melillo & Aber, 1982; Harmon *et al.*, 1990). Because the 'best' two models were not ecologically realistic, we used the next (third) best model to estimate initial pool sizes (model #3 in Table 7). In this model, as the L/N ratio increases, the size of the M_1 pool decreases (conversely M_2 increases) rapidly at first, but then changes more slowly as the L/N approaches 60, after which the pool sizes remain constant.

H4: A composite climate variable that incorporates the effects of temperature and soil moisture better represented the effect of climate on decomposition than variables that did not

Of the four climate models included in set 1, AICc selected the model that used CDI_{exp} as the best model (Table 8). The model that used CDI_{exp} had the only $\Delta r < 10$, indicating that it had substantial support in the LIDET dataset and was a significant improvement over AET, PET, MAT, and MAP.

H5: Across ecosystems, the effects of temperature on decomposition were best represented by a variable Q_{10} function

Although all models that used CDIs (and converged) were better than models that used more traditional climatic descriptors, the CDIs that used variable Q_{10} temperature functions (CDI_{atan}, CDI_{LT}, CDI_{DEFAC}, and CDI_K) substantially improved the ability of our model to predict long-term decomposition at large scales (Table 8). In combination with the best initial pool model from H3, AICc selected CDI_{LT} as the climate descriptor that best represented the effect of climate on decomposition across all sites (Table 8, Fig. 3).

However, because CDI_{atan} was a relatively close competitor to CDI_{LT}, we reanalyzed the H1–H3 model sets using CDI_{atan}. The results for H1 and H2 were the same, and the results for H3 were very similar, with the best models producing unrealistic decomposition parameters and maximum pool sizes for $M_2 + M_3$ (data not shown). The first realistic model for H3 was the same model that was chosen using CDI_{LT}, but using CDI_{LT} produced a better fit than CDI_{atan} (best H3 model with CDI_{LT} $\Delta r = 0$, with CDI_{atan} $\Delta r = 8.58$, data not shown).

This final climate model (the best initial pool model from H3 with CDI_{LT}) was the overall best model for describing the decomposition of all litter species and types at all sites in the LIDET dataset. This relatively simple model explained 68% of the variation in long-term litter decomposition in diverse ecosystems across two continents.

Systematic biases due to litter type, site, and ecosystem differences

We investigated different litter types, sites, and biomes for systematic deviations from the predictions of the overall best model. In most cases, we used AICc to investigate the observed deviations. Some of these statistical investigations were *post hoc* – in these cases, we do not suggest that inferences regarding model-selection uncertainty and extrapolation to new datasets are statistically robust. Nonetheless, these investigations revealed several cases where our model tended to consistently over- or underpredict decomposition, which appeared to be driven by differences in litter type, biome, or local environments.

Litter type – above- vs. belowground decomposition. Use of AICc to compare the overall best model for all litter types with a model that estimated separate decomposition constants (k_ps) for roots and leaf litter (Table 9) indicated that the litter separate model was clearly the better model (Table 9).

Site and biome biases. Litter mass loss in wetlands (NIN and VCR) was not well-predicted by our model (Fig. 4). Over the entire experimental period, the best overall model overpredicted leaf litter remaining by an average of 7%, but underpredicted the amount of root litter that remained by an average of 32%. Because belowground decomposition was particularly poorly described, we compared the best overall model to a model that estimated separate k_ps for all litter at wetland sites and a model that estimated separate k_ps for only root litter at wetland sites. Separating litter at wetland sites from the litter at other sites decreased the AICc of the model, but separating only the wetland roots from the rest of the data resulted in the best model (Table 10). The selection of the wetland root model and the considerably different wetland root k_p values compared to the k_p values of all other litter indicated that root litter in wetland sites had substantially different decomposition dynamics from all other litter (Fig. 4).

Belowground decomposition in alpine and arctic sites (ARC, NWT, and LVW) was 10% slower than was

Table 8 The best model from hypothesis 3 (the initial pool models) was used to determine which climate decomposition index (CDI) best predicted decomposition at the LIDET (Long-term Intersite Decomposition Experiment Team) sites

CDI	Climate model set #	N	R^2	P	AICc	Overall Δr	Set 1 Δr	Set 2 Δr	w_r	k_1	k_2	k_3	b	β_1	β_2
Exponential (CDI_{exp})	1, 2	2039	0.615	<0.0001	10 945.4	382.8	0	382.8	0.000	2.1287	0.4236	0.0043	1.959	64.39	0.020
AET	1	2039	0.535	<0.0001	11 327.3	764.7	381.9	–	0.000	0.0021	0.0003	0.0000	1.513	63.70	0.020
MAP	1	2039	0.524	<0.0001	11 374.6	812.0	429.2	–	0.000	0.0017	0.0002	0.0000	1.396	66.05	0.019
PET	1	2039	0.301	<0.0001	11 782.8	1220.2	837.4	–	0.000	0.0030	0.0002	0.0000	1.091	53.82	0.020
MAT	1	2039	0.418	<0.0001	14 234.9	3672.3	3289.5	–	0.000	0.0146	0.0496	0.0140	0.879	100.00	0.001
Linear (CDI_{linear})*	1, 2	2039													
Lloyd and Taylor (CDI_{LT})	2	2039	0.680	<0.0001	10 562.6	0.0	–	0	0.986	3.5454	0.7471	0.0270	1.324	57.17	0.030
Arctangent (CDI_{atan})	2	2039	0.679	<0.0001	10 571.2	8.6	–	8.6	0.014	6.1399	1.2805	0.0584	1.315	57.01	0.031
CENTURY (CDI_{DEFAC})	2	2039	0.672	<0.0001	10 617.6	55.0	–	55.0	0.000	4.0373	0.8387	0.0190	1.504	58.73	0.026
Kirschbaum (CDI_K)	2	2039	0.663	<0.0001	10 675.3	112.7	–	112.7	0.000	2.8786	0.5993	0.0123	1.586	59.98	0.025

Climate model set #1 tested noncomposite vs. composite climate indices (hypothesis 4). Climate model set #2 tested CDIs with constant Q_{10} temperature functions vs. those with variable Q_{10} temperature functions (hypothesis 5). The asterisk denotes that the model using CDI_{linear} failed to converge, so parameter estimates and model statistics are not given. CDI_{LT} best described the effect of climate on decomposition at the LIDET sites and was the best overall model.
MAP, mean annual precipitation; MAT, mean annual temperature; AET, actual evapotranspiration; PET, potential evapotranspiration.

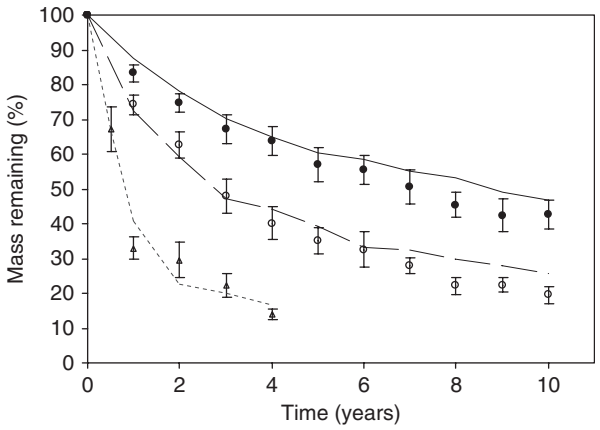

Fig. 3 Climate modifies decomposition rates in the observed LIDET (Long-term Intersite Decomposition Experiment Team) data and model predictions from the best overall model (from hypothesis 5). Predictions and observed data are averaged across all litter types. Decomposition proceeds most slowly at an arctic site (ARC, solid circles and line), at moderate rates in a temperate forest site (AND, open circles and dashed line), and very quickly at a wet tropical forest site (LBS, open triangles and dotted line). Symbols are observed data. Lines are model predictions. Error bars are ±1 SE.

predicted by the best overall model. In contrast, aboveground litter decomposition was <1% slower than predicted over the entire experimental period. Because our model accurately described decomposition aboveground but not belowground, we used AICc to compare the best overall model with a model that estimated separate k_ps for the roots in these ecosystems. Of these two models, AICc chose the model that estimated separate k_ps for arctic roots as the best model (Table 11 and Fig. 5). In general, the k_ps for arctic roots were lower than those for either the remaining litter types or the best overall model.

In temperate deciduous forests (HBR, HFR, and CWT) and moist to humid tropical sites (BCI, LUQ, LBS, and MTV), aboveground litter decomposed more rapidly than predicted, particularly if the litter was of high quality (low L/N and L/cell ratios). Across the entire sampling period, the best overall model underpredicted leaf litter mass loss in temperate deciduous and moist tropical ecosystems by an average of 6%. Tropical forests on highly weathered soils typically have high rates of N cycling and availability relative to other ecosystems (Reich *et al*., 1997; Martinelli *et al*., 1999; Booth *et al*., 2005); thus, we hypothesized that the elevated decomposition rates may be due to higher levels of N in soils or site litter, which supplemented the N in each litter type, thus increasing decomposition rates (Vitousek, 1994; Ostertag & Hobbie, 1999; Hobbie & Vitousek, 2000). The temperate deciduous sites are likely

Table 9 Estimating separate parameters for leaf and root litter ('Litter separate') using the best model from hypothesis 4 was better supported by the LIDET (Long-term Intersite Decomposition Experiment Team) dataset

Model	N	R^2	P	AICc	Δr	w_r	k_1 or k_{1L}	k_2 or k_{2L}	k_3 or k_{3L}	k_{1R}	k_{2R}	k_{3R}	b	β_1	β_2
Litter separate	2039	0.693	<0.0001	10490	0	1.0	3.170	0.834	0.053	5.572	0.614	0.022	1.507	57.167	0.030
Litter together	2039	0.680	<0.0001	10563	69	1.1E-15	3.545	0.747	0.027				1.324	57.167	0.030
k_{iR}/k_{iL}							1.758	0.736	0.417						

Comparing k_is for root and leaf litter by pool indicated that the belowground labile pool decomposed more rapidly, but the more recalcitrant pools (M_2 and M_3) decayed more slowly than aboveground litter. The 'litter together' model is the best overall model derived from hypothesis 5 (Table 8). Subscripts L and R are leaf and root.

to be impacted by anthropogenic N deposition (Swank & Vose, 1997; Aber *et al.*, 1998; CASTNET, 2005), which could increase early rates of decomposition at these sites by elevating litter N and/or inorganic N availability (Fenn, 1991; Kuperman, 1999; Knorr *et al.*, 2005; Bragazza *et al.*, 2006). To investigate this idea, we derived a set of equations that acted to increase the initial N concentration of the litter and, thus the size of the labile C pool (Appendix A). These equations create an N multiplier, which decreases the L/N ratio by multiplying the initial litter N concentration by a positive number calculated as a function of the L/cellulose (L/cell) ratio. The equations increased initial N by a large and constant amount for litter with low L/cell ratios (L/cell < 0.2, N multiplier = 5) and by a small and constant amount (N multiplier = 2) for litter with high L/cell (> 0.4). Between these two values, the value of the N multiplier decreases linearly. Fitting this equation to the aboveground leaf litter at tropical and temperate deciduous forest sites increased the ability of the model to predict mass loss at these sites ($\Delta r = 0$, $w_r = 1$ for this model fit to temperate and tropical aboveground litter, vs. $\Delta r = 74$, $w_r = 9.9 \times 10^{-22}$ for the overall best model fit to the same data, Fig. 6).

At the very arid sites (JRN, CPR, SEV), belowground decomposition and initial rates of aboveground litter decomposition were relatively well-predicted by the best overall model. However, after 3–5 years, mass loss of aboveground litter was faster than predicted by climate and initial litter quality (Fig. 7). For the first 5 years of the experimental period, the best overall model underpredicted decomposition of aboveground litter by <1%. By the end of the experiment, aboveground decomposition was underpredicted by 25% on average. The long-term decomposition trends over time also followed an atypical pattern, loosing mass linearly over time (Fig. 7).

We identified two additional sites where our model substantially under- or overpredicted decomposition. Because these trends were only present at two sites, with potentially different abiotic drivers, we did not statistically analyze these trends. At OLY, a temperate site that receives very high levels of precipitation

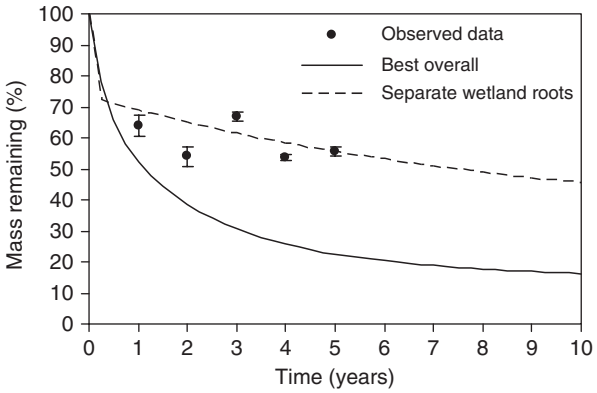

Fig. 4 Predicting root decomposition at wetland sites is greatly improved by estimating decomposition rates of wetland roots (k_{pW}) separately from all other litter (leaf and root) in the LIDET (Long-term Intersite Decomposition Experiment Team) dataset (dashed line). Model predictions and observed data are averaged across all species. Root decomposition at the wetland site NIN is poorly predicted by the best overall model (solid line), which estimates decomposition rates for all litter together. Solid circles are observed root-litter data at NIN. Error bars are ±1 SE.

(Table 1), the model overpredicted the amount of mass remaining at the end of the 10-year sampling period by 7%, meaning that decomposition was faster than predicted. In contrast, the model described mass loss of root litter fairly accurately (predicted mass remaining was 1% more than the observed mass remaining). At BSF, a temperate coniferous forest with a particularly seasonal weather pattern, decomposition was slower than predicted for both above- and belowground litter. At the end of the experimental period, the best overall model underestimated the litter mass remaining at BSF by approximately 13%, indicating that our model may not accurately depict decomposition at sites with extremely seasonal precipitation patterns.

Discussion

Model structure and litter quality (H1–H3)

Model selection of the three-pool model was consistent with our initial hypothesis (H1). Although short-term

Table 10 Estimating separate parameters for wetlands (wetlands separate), but particularly for wetland roots (wetland roots separate), more accurately depicted decomposition at the LIDET (Long-term Intersite Decomposition Experiment Team) sites

Model	N	R^2	P	AICc	Δr	w_r	k_1 or k_{1T}	k_2 or k_{2T}	k_3 or k_{3T}	k_{1W}	k_{2W}	k_{3W}	b	β_1	β_2
Wetland roots separate	2039	0.712	<0.0001	10353	0	1.000	3.486	0.805	0.045	3544	0.036	0.177	1.59	57.17	0.03
Wetlands separate	2039	0.683	<0.0001	10552	200	3.3E-44	3.558	0.743	0.041	4.645	0.665	0	1.37	57.17	0.03
All sites	2039	0.680	<0.0001	10563	210	0.000	3.545	0.747	0.027				1.32	57.17	0.03

The 'all sites' model is the best overall model derived from hypothesis 5 (Table 8). Subscripts T and W are terrestrial and wetland.

Table 11 Estimating separate parameters for the decomposition of roots in the arctic (arctic roots separate), more accurately depicted decomposition across all the LIDET (Long-term Intersite Decomposition Experiment Team) sites

Model	N	R^2	P	AICc	Δr	w_r	k_1 or k_{1A}	k_2 or k_{2A}	k_3 or k_{3A}	k_{1NA}	k_{2NA}	k_{3NA}	b	β_1	β_2
Arctic roots separate	2039	0.689	<0.0001	10516	0	1	3.936	0.307	0.012	3.649	0.788	0.025	1.406	57.167	0.030
All sites	2039	0.680	<0.0001	10563	210	0.000	3.545	0.747	0.027				1.324	57.167	0.030

The 'all sites' model is the best overall model derived from hypothesis 5 (Table 8). Subscripts A and NA are arctic roots and nonarctic litter.

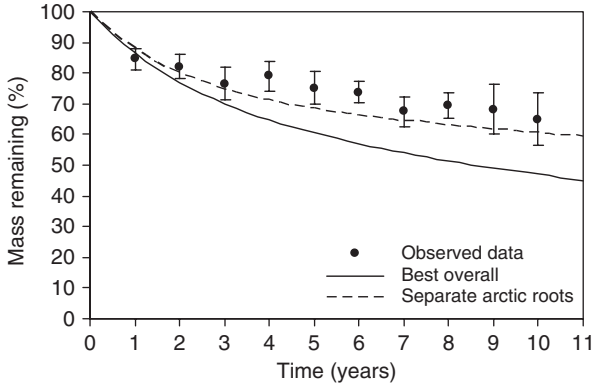

Fig. 5 Root decomposition at arctic and alpine sites was slower than predicted by the best overall model. Observed data and predictions are averaged across species. Description of root decomposition at arctic and alpine sites was improved by estimating separate k_ps for root litter at these sites. Error bars are ±1 SE.

litter decomposition studies have found litter decomposition to be adequately described by single-pool models (e.g. Trofymow *et al*., 2002; S. E. Hobbie, Litter decomposition study, unpublished data), long-term decomposition rates are often better described by multiple-pool models (Bunnell & Tait, 1974; Wieder & Lang, 1982). Our results indicate that for long-term decomposition, two- and three-pool models are significant improvements over a one-pool model. This suggests that as litter decomposes, the chemical (litter chemistry), biological, and physical characteristics and processes that control its decomposition may vary.

In the best litter quality model (H2), the maximum decomposition rate of M_2 was decreased exponentially by increasing the lignin fraction (Table 3), such that as the amount of lignin relative to cellulose increased, the size of the lignin-encrusted cellulose pool also increased (Berg *et al*., 1984; Aber *et al*., 1990). Thus, the decomposition of cellulose (M_2) is increasingly controlled by the decomposition rate of lignin, which must be decomposed to gain access to cellulose (Berg *et al*., 1982; Aber *et al*., 1990). Accordingly, the best litter quality model decreased the decomposition rate of M_2 as the initial lignin fraction increased. Overall, the effect of litter quality can be seen at all the sites, regardless of climate (Fig. 2). These results are consistent with our second hypothesis, that C quality influences the decomposition rate of 'slow' pools through lignin protection of cellulose.

Using the L/N ratio to estimate initial pool sizes significantly improved the ability of our model to predict mass loss over time. All of the models that used L/N ratios to estimate pool sizes were better than the model that used measured C chemistry. Thus, our results are consistent with research that has found high litter N concentrations to increase initial rates of decomposition (Berg *et al*., 1982; Hobbie, 2005), and with our hypothesis that litter with low initial L/N ratios decomposes more quickly initially than litter with high L/N ratios.

In contrast, using estimated cellulose (M_2) in the litter quality modifier of the second pool (L_s) did not improve the model. This suggests that, while N affected initial decomposition rates by modifying the size of the M_1 (labile) pool, it did not have a similar effect on the

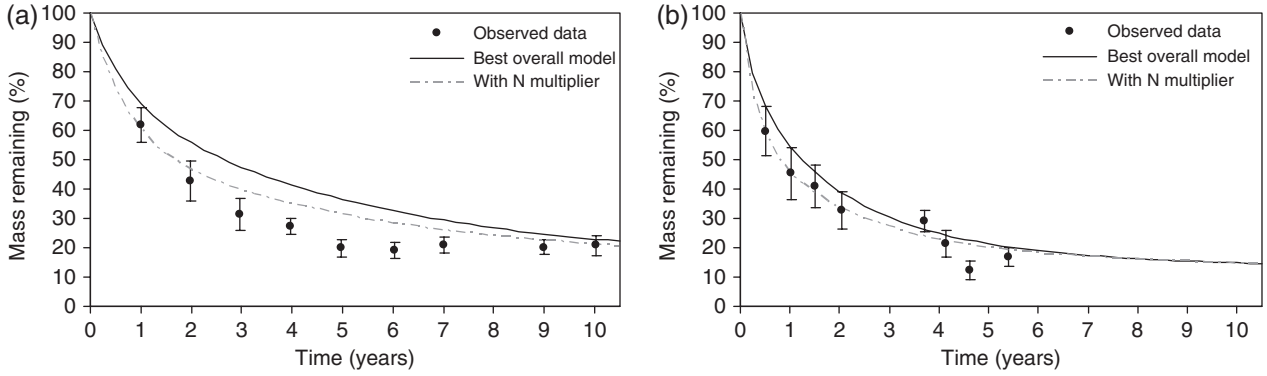

Fig. 6 Decomposition of aboveground leaf litter (averaged over main species aboveground litter types) is fairly well-described by the best overall model (hypothesis 5, H5; solid line) at (a) HFR, a temperate deciduous forest and (b) MTV, a moist tropical forest, but predictions of decomposition are improved by using an 'effective initial N concentration' at temperate and tropical sites (dashed line). The main effect of using this factor is to increase initial decomposition rates. Error bars are ±1 SE.

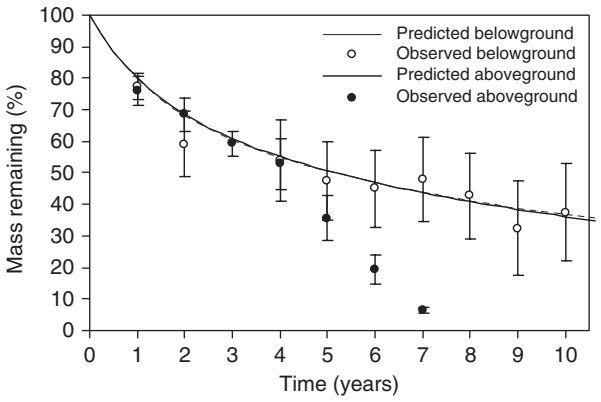

Fig. 7 Near-linear decay of aboveground leaf litter at JRN. Observations and predictions are averaged across all litter species. Initial rates are slightly slower than predicted, but decay continues at similar rates as decomposition continues, so that mass loss is greater than predicted by year 5. Root-litter decomposition at JRN follows the more traditional pattern of decomposition predicted by our model. Error bars are ± 1 SE.

slower phase of decomposition, which was primarily affected by the lignin fraction, L_s. Thus, the decomposition of the cellulose fraction, free and lignin-encrusted, may not be as favorably influenced by litter N content as the labile pool. This is in line with our hypotheses that while fast decomposition would be influenced by N concentration (through the L/N ratio, H3), slow decomposition rates would be primarily influenced by litter C chemistry (H2).

Climate effects on large-scale patterns of decomposition (H4 and H5)

For the previous hypotheses, we assumed that a CDI with a variable Q_{10} temperature function would be a good descriptor of how climate affects decomposition (Del Grosso *et al*., 2005). We tested this assumption with two separate predictions and model subsets. H4 addresses the use of a composite climate index and H5 addresses the inclusion of a variable Q_{10} temperature function into CDIs.

Incorporating temperature and water-stress effects on decomposition by using a CDI improved the ability of the litter quality model to describe long-term decomposition across a wide range of climates vs. more traditional climate descriptors such as MAT, MAP, and AET (H4; Table 8). This is consistent with an analysis of the short-term LIDET results by Gholz *et al*. (2000), who also found a composite variable (CDI_{DEFAC}) to be a better predictor of climatic effects on decomposition than AET, MAT, or MAP.

As we hypothesized (H5), the CDIs that used variable Q_{10} functions further improved the litter quality model's ability to describe decomposition in the LIDET dataset. The model with CDI_{LT} was selected as the best climate model, resulting in the best overall model (Table 8). This contrasts with the results of Del Grosso *et al*. (2005) who found CDI_{atan} best described the effect of climate in a metadata analysis of heterotrophic respiration (winter soil respiration data) and soil respiration from temperate systems (including root respiration). However, CDI_{LT} was a close second to CDI_{atan}, particularly when respiration was primarily heterotrophic (Del Grosso *et al*., 2005). Because litter decomposition is a heterotrophic process, the selection of CDI_{LT} in our analysis may indicate that this variable better represents climatic control over heterotrophic respiration. Alternatively, it may be a result of the greater range of climates and site characteristics included in the LIDET dataset, as CDI_{LT} is typically higher in both cold and very warm environments than CDI_{atan} (Del Grosso *et al*., 2005).

Systematic biases

As we expected, we found several systematic deviations from our best overall model predictions based on litter type and biome or ecosystem type. Above- and belowground litter decomposed at different rates and some biome-specific environments were not well-represented by our model: very wet conditions at temperate sites, cold soils, seasonal weather patterns with uneven distribution of precipitation, and possibly N-rich temperate and tropical sites. Additionally, decomposition of aboveground litter at arid sites did not follow the pattern predicted by our negative exponential decomposition model, suggesting that different processes may be controlling long-term decomposition at these sites.

Litter type

Estimating separate decomposition constants for root and leaf litter substantially improved the model's ability to describe mass loss in the LIDET dataset. Examining the decomposition constants for the leaf and root litter for all three pools indicated that while root litter decomposed more quickly than leaf litter during initial decomposition, it decomposed more slowly during the later stages of decomposition (Table 9). This could be due to greater levels of N availability and labile C (e.g. rhizodeposits) belowground that may increase rates of slow/lignin decomposition (Berg & Ågren, 1984; Melillo *et al*., 1989), or an ameliorated climate that maintains longer periods of adequate moisture and temperature. Our results are consistent with the results of Chen *et al*. (2001), who examined fine root decomposition over 2 years.

Biome-specific biases

As could be expected with any general large-scale model, specific conditions at specific sites were not particularly well-represented. In wetlands, estimating separate k_ps for wetland roots resulted in a better fit to the LIDET data. Initial decomposition rates for roots at wetland sites were extremely high (k_{1W}), suggesting that the loss of soluble compounds belowground was very rapid. Perhaps due to anaerobic conditions, decomposition of the remaining wetland root material was much slower than for all other litter and decomposition of the recalcitrant pool was essentially zero ($k_{3W} = 0$, Table 10, Fig. 4; Trofymow *et al*., 2002). High levels of litter leaching may also explain the higher-than-predicted rates of above- and belowground decomposition at OLY, which has a MAP as high as wet tropical systems (Table 1) but a temperate thermal regime.

In arctic and alpine environments, roots decomposed much more slowly than the best overall model predicted (Fig. 5). Cold summer soils may limit belowground decomposition by decreasing decomposer activity and limiting nutrient cycling and availability. For the sites with available data (four of five sites), average June–August soil temperatures were between 3 and 9°C, which is 1.1–6.1°C colder than air temperatures for the same period. The average May–August soil temperature at temperate sites is much warmer (e.g. at CDR = 20°C).

Decomposition at BSF, a site with strong seasonal precipitation patterns, was slower than predicted for both above- and belowground litter. Although MAP and CDI_{LT} are relatively high for this site, it has a particularly dry summer. A summer drought index that subtracts mean May–September PET from total precipitation (Liski *et al*., 2003) for the experimental period clearly shows that BSF has a dry growing season when compared with sites with similar CDI_{LT}s. This index puts BSF in the same range as semiarid sites (e.g. CPR; Table 1). Hart *et al*. (1992) also found that decomposition at this site was likely limited by the temporal separation of high temperatures and precipitation. The overestimation of mass loss by our model suggests that CDI_{LT} was unable to capture the effect of this extreme seasonal variation on decomposition.

Decomposition at temperate deciduous and wet tropical sites was somewhat faster than predicted. Our analyses showed that the N multiplier increased the ability of the best overall model to predict mass loss (Fig. 6), suggesting that external sources of N may be enhancing initial decomposition at these sites. There may be other explanations for the fast decomposition at these sites, and future investigations of decomposition at such sites should test our N availability hypothesis against other relevant hypotheses.

The near-linear decomposition of aboveground litter at the arid sites was poorly described by the best overall model (Fig. 7). The arid climates at these sites result in low primary productivity and canopy cover (Parton *et al*., 2007). Leaf litter at these sites, therefore, experiences higher levels of UV radiation than litter at more humid or forested sites. The unexpected linear pattern of leaf decomposition that we observed at these sites may, therefore, be a result of photodegradation. Exposure to high levels of UV is thought to directly influence decomposition by negatively affecting the decomposer communities (Newsham *et al*., 1997; Duguay & Klironomos, 2000; Moody *et al*., 2001; Pancotto *et al*., 2003) and/or by positively affecting the mass loss through photochemical litter breakdown (Gehrke *et al*., 1995; Rozema *et al*., 1997; Pancotto *et al*., 2005; Austin & Vivanco, 2006). Recent work suggests that in arid environments where biotic decomposition is not favored,

UV-related decomposition may control rates of litter mass loss (Pancotto *et al*., 2005; Parton *et al*., 2007). Indeed, Austin & Vivanco (2006) found UV-controlled litter decomposition patterns that are strikingly similar to the patterns of decomposition that we observed at these sites.

Conclusions

We were able to describe long-term rates of decomposition in a wide range of ecosystems and climates using a relatively simple model based on site climate and the initial litter quality characteristics of each litter type. Litter was divided into three initial pools based on the initial L/N ratio and lignin content of each litter. The decomposition of the intermediate litter pool was modified by the initial lignin and cellulose contents. Decomposition of all three pools was influenced by climate, and a composite climate variable that used Lloyd & Taylor's (1994) variable Q_{10} function predicted the effect of climate on decomposition more accurately than AET or five other alternative composite climate variables.

While there were notable systematic deviations from the model predictions, these deviations were largely due to litter type, site, or biome-specific differences, which our model was too simple to capture. In spite of these deviations, our model was able to describe a large fraction of the variation in the decomposition of a wide range of litter types across extremely variable climates (68% or 72% excluding wetland sites, data not shown). The overall success of our model in matching global trends in decomposition has large implications for simulation models that attempt to predict long-term changes in global C cycling. Future tests of our model against new datasets will assess the general predictive ability of this model and clarify the systematic departures from model predictions that we observed in the LIDET dataset.

Acknowledgements

We thank the LIDET teams at all sites for logistical and technical support and B. Fasth for analysis. NSF grants DEB-0322057, DEB-0080382, DEB-0218039, DEB-0219104, DEB-0217631 (Bio-Complexity and Cedar Creek, Shortgrass Steppe, Cedar Creek, Andrews, and Luquillo Long-Term Ecological Research projects), DEB-0425908 and 0416223, and by the Colorado Agricultural Experiment Station (MS-55353) and the California Agricultural Experiment Station (MS-7069).

References

Aber JD, McDowell W, Nadelhoffer K *et al*. (1998) Nitrogen saturation in temperate forest ecosystems. *Bioscience*, **48**, 921–934.

Aber JD, Melillo JM, McClaugherty CA (1990) Predicting long-term patterns of mass-loss, nitrogen dynamics, and soil organic-matter formation from initial fine litter chemistry in temperate forest ecosystems. *Canadian Journal of Botany – Revue Canadienne De Botanique*, **68**, 2201–2208.

Ågren GI, McMurtrie RE, Parton WJ, Pastor J, Shugart HH (1991) State-of-the-art of models of production decomposition linkages in conifer and grassland ecosystems. *Ecological Applications*, **1**, 118–138.

Allen RG, Perieira LS, Raes D, Smith M (1998) *Crop Evapotranspiration – Guidelines for Computing Crop Water Requirements*. Food and Agriculture Organization of the United Nations, Rome.

Austin AT, Vivanco L (2006) Plant litter decomposition in a semiarid ecosystem controlled by photodegradation. *Nature*, **442**, 555–558.

Berg B, Ågren GI (1984) Decomposition of needle litter and its organic-chemical components – theory and field experiments – long-term decomposition in a Scots pine forest. 3. *Canadian Journal of Botany – Revue Canadienne De Botanique*, **62**, 2880–2888.

Berg B, Ekbohm G, McClaugherty C (1984) Lignin and holocellulose relations during long-term decomposition of some forest litters – long-term decomposition in a Scots pine forest. 4. *Canadian Journal of Botany – Revue Canadienne De Botanique*, **62**, 2540–2550.

Berg B, Hannus K, Popoff T, Theander O (1982) Changes in organic-chemical components of needle litter during decomposition – long-term decomposition in a Scots Pine forest. 1. *Canadian Journal of Botany – Revue Canadienne De Botanique*, **60**, 1310–1319.

Booth MS, Stark JM, Rastetter E (2005) Controls on nitrogen cycling in terrestrial ecosystems: a synthetic analysis of literature data. *Ecological Monographs*, **75**, 139–157.

Bragazza L, Freeman C, Jones T *et al*. (2006) Atmospheric nitrogen deposition promotes carbon loss from peat bogs. *Proceedings of the National Academy of Sciences*, **103**, 19386–19389.

Bunnell FL, Tait DEN (1974) Mathematical simulation models of decomposition processes. In: *Soil Organisms and Decomposition in the Tundra* (eds Holding AJ, Heal OW, Maclean SFJ, Flanagan PW), pp. 207–225. International Biological Programme, Tundra Biome Steering Committee, Stockholm, Sweden.

Burke IC, Kaye JP, Bird SP, Hall SA, McCulley RL, Sommerville GL (2003) Evaluating and testing models of terrestrial biogeochemistry: the role of temperature in controlling decomposition. In: *Models in Ecosystem Science* (eds Canham CD, Lauenroth WK), pp. 225–253. Princeton University Press, Princeton, NJ.

Burnham KP, Anderson DR (2002) *Model Selection and Multimodel Inference: A Practical Information-Theoretic Approach*. Springer-Verlag, New York.

Chen H, Harmon ME, Griffiths RP (2001) Decomposition and nitrogen release from decomposing woody roots in coniferous forests of the Pacific Northwest: a chronosequence approach. *Canadian Journal of Forest Research – Revue Canadienne De Recherche Forestiere*, **31**, 246–260.

Chesson A (1997) Plant degradation by ruminants: parallels with litter decomposition in soils. In: *Driven by Nature: Plant Litter Quality and Decomposition* (eds Cadisch G, Giller KE), pp. 47–66. CAB International, Wallingford.

Corbeels M, McMurtrie RE, Pepper DA, O'Connell AM (2005) A process-based model of nitrogen cycling in forest plantations Part I. Structure, calibration and analysis of the decomposition model. *Ecological Modelling*, **187**, 426–448.

Del Grosso SJ, Parton WJ, Mosier AR, Holland EA, Pendall E, Schimel DS, Ojima DS (2005) Modeling soil CO2 emissions from ecosystems. *Biogeochemistry*, **73**, 71–91.

Duguay KJ, Klironomos JN (2000) Direct and indirect effects of enhanced UV-B radiation on the decomposing and competitive abilities of saprobic fungi. *Applied Soil Ecology*, **14**, 157–164.

Fenn M (1991) Increased site fertility and litter decomposition rate in high pollution sites in the San Bernadino Mountains. *Forest Science*, **37**, 1163–1181.

Gehrke C, Johanson U, Callaghan TV, Chadwick D, Robinson CH (1995) The impact of enhanced ultraviolet-b radiation on litter quality and decomposition processes in Vaccinium leaves from the sub-arctic. *Oikos*, **72**, 213–222.

Gholz HL, Wedin DA, Smitherman SM, Harmon ME, Parton WJ (2000) Long-term dynamics of pine and hardwood litter in contrasting environments: toward a global model of decomposition. *Global Change Biology*, **6**, 751–765.

Harmon ME, Baker GA, Spycher G, Greene SE (1990) Leaf-litter decomposition in the Picea-Tsuga forests of Olympic National-Park, Washington, USA. *Forest Ecology and Management*, **31**, 55–66.

Hart SC, Firestone MK, Paul EA (1992) Decomposition and nutrient dynamics of ponderosa pine needles in a Mediterranean-type climate. *Canadian Journal of Forest Research*, **22**, 306–314.

Hobbie SE (2005) Contrasting effects of substrate and fertilizer nitrogen on the early stages of litter decomposition. *Ecosystems*, **8**, 644–656.

Hobbie SE, Gough L (2004) Litter decomposition in moist acidic and non-acidic tundra with different glacial histories. *Oecologia*, **140**, 113–124.

Hobbie SE, Vitousek PM (2000) Nutrient limitation of decomposition in Hawaiian forests. *Ecology*, **81**, 1867–1877.

Hutchinson KJ, King KL, Nicol GR, Wilkinson DR (1990) Methods for evaluating the role of residues in the nutrient cycling economy of pastures. In: *Nutrient Cycling in Terrestrial Ecosystems Field Methods. Application and Interpretation* (eds Harrison AF, Ineson P, Heal OW), pp. 291–314. Elsevier Applied Science, Amsterdam.

Kirschbaum MUF (1995) The temperature-dependence of soil organic-matter decomposition, and the effect of global warming on soil organic-C storage. *Soil Biology & Biochemistry*, **27**, 753–760.

Kirschbaum MUF (2006) The temperature dependence of organic-matter decomposition – still a topic of debate. *Soil Biology & Biochemistry*, **38**, 2510–2518.

Knorr M, Frey SD, Curtis PS (2005) Nitrogen additions and litter decomposition: a meta-analysis. *Ecology*, **86**, 3252–3257.

Kuperman RG (1999) Litter decomposition and nutrient dynamics in oak-hickory forests along a historic gradient of nitrogen and sulfur deposition. *Soil Biology and Biochemistry*, **31**, 237–244.

Kurz-Besson C, Coûteaux M, Thiéry JM, Berg B, Remacle J (2005) A comparison of litterbag and direct observation methods of Scots pine needle decomposition measurement. *Soil Biology and Biochemistry*, **37**, 2315–2318.

Liski J, Nissinen A, Erhard M, Taskinen O (2003) Climatic effects on litter decomposition from arctic tundra to tropical rainforest. *Global Change Biology*, **9**, 575–584.

Lloyd J, Taylor JA (1994) On the temperature-dependence of soil respiration. *Functional Ecology*, **8**, 315–323.

Long-term Intersite Decomposition Experiment Team (LIDET) (1995) *Meeting the Challenges of Long-Term, Broad Scale Ecological Experiments*. U.S. LTER Network Office, Seattle, WA.

Luckai N, Larocque GR (2002) Challenges in the application of existing process-based models to predict the effect of climate change on C pools in forest ecosystems. *Climatic Change*, **55**, 39–60.

Martinelli LA, Piccolo MC, Townsend AR *et al*. (1999) Nitrogen stable isotopic composition of leaves and soil: tropical versus temperate forests. *Biogeochemistry*, **46**, 45–65.

McClaugherty C, Berg B (1987) Cellulose, Lignin and Nitrogen concentrations as rate regulating factors in late stages of forest litter decomposition. *Pedobiologia*, **30**, 101–112.

McGuire AD, Melillo JM, Kicklighter DW *et al*. (1997) Equilibrium responses of global net primary production and carbon storage to doubled atmospheric carbon dioxide: sensitivity to changes in vegetation nitrogen concentration. *Global Biogeochemical Cycles*, **11**, 173–189.

McGuire AD, Melillo JM, Kicklighter DW, Joyce LA (1995) Equilibrium responses of soil carbon to climate change: empirical and process-based estimates. *Journal of Biogeography*, **22**, 785–796.

Meentemeyer V (1978) Macroclimate and lignin control of litter decomposition rates. *Ecology*, **59**, 465–472.

Melillo JM, Aber JD (1982) Nitrogen and lignin control of hardwood leaf litter decomposition dynamics. *Ecology*, **63**, 621–626.

Melillo JM, Aber JD, Linkins AE, Ricca A, Fry B, Nadelhoffer KJ (1989) Carbon and nitrogen dynamics along the decay continuum – plant litter to soil organic-matter. *Plant and Soil*, **115**, 189–198.

Minderman G (1968) Addition, decomposition and accumulation of organic matter in forest. *Journal of Ecology*, **56**, 355–362.

Moody SA, Paul ND, Björn LO *et al*. (2001) The direct effects of UV-B radiation on *Betula pubescens* litter decomposing at four European field sites. *Plant Ecology*, **154**, 27.

Moorhead DL, Currie WS, Rastetter EB, Parton WJ, Harmon ME (1999) Climate and litter quality controls on decomposition: an analysis of modeling approaches. *Global Biogeochemical Cycles*, **13**, 575–589.

Newsham KK, McLeod AR, Roberts JD, Greenslade PD, Emmett BA (1997) Direct effects of elevated UV-B radiation on the decomposition of Quercus robur leaf litter. *Oikos*, **79**, 592–602.

Olson JS (1963) Energy storage and balance of producers and decomposers in ecological systems. *Ecology*, **44**, 322.

Ostertag R, Hobbie SE (1999) Early stages of root and leaf decomposition in Hawaiian forests: effects of nutrient availability. *Oecologia*, **121**, 564–573.

Pancotto VA, Sala OE, Cabello M *et al*. (2003) Solar UV-B decreases decomposition in herbaceous plant litter in Tierra

del Fuego, Argentina: potential role of an altered decomposer community. *Global Change Biology*, **9**, 1465–1474.

Pancotto VA, Sala OE, Robson TM, Caldwell MM, Scopel AL (2005) Direct and indirect effects of solar ultraviolet-B radiation on long-term decomposition. *Global Change Biology*, **11**, 1982–1989.

Pan YD, Melillo JM, McGuire AD *et al*. (1998) Modeled responses of terrestrial ecosystems to elevated atmospheric CO2: a comparison of simulations by the biogeochemistry models of the Vegetation/Ecosystem Modeling and Analysis Project (VEMAP). *Oecologia*, **114**, 389–404.

Parton WJ, Cole CV, Stewart JWB, Ojima DS, Schimel DS (1989) Simulating regional patterns of soil C, N, and P dynamics in the U.S. central grasslands region. In: *Ecology of Arable Land* (eds Clarholm M, Bergström L), pp. 99–108. Kluwer Academic Publishers, Dordrecht.

Parton WJ, Schimel DS, Cole CV, Ojima DS (1987) Analysis of factors controlling soil organic-matter levels in Great-Plains Grasslands. *Soil Science Society of America Journal*, **51**, 1173–1179.

Parton WJ, Schimel DS, Ojima DS, Cole CV (1994) A general model for soil organic matter dynamics. In: *Sensitivity to Litter Chemistry, Texture and Management, Quantitative Modeling of Soil Forming Processes* (eds Bryant RB, Arnold RW), pp. 137–167. Soil Science Society of America Special Publication, Madison, WI.

Parton W, Silver WL, Burke IC *et al*. (2007) Global-scale similarities in nitrogen release patterns during long-term decomposition. *Science*, **315**, 361–364.

Potter CS, Randerson JT, Field CB, Matson PA, Vitousek PM, Mooney HA, Klooster SA (1993) Terrestrial ecosystem production - a process model based on global satellite and surface data. *Global Biogeochemical Cycles*, **7**, 811–841.

Prentice IC, Farquhar GD, Fasham MJR *et al*. (2001) The carbon cycle and atmospheric carbon dioxide. In: *Climate Change 2001: the Scientific Basis. Contribution of Working Group I to the Third Assessment Report of the Intergovernmental Panel on Climate Change* (eds Houghton JT, Ding Y, Griggs DJ *et al*.), pp. 183–237. Cambridge University Press, Cambridge, UK.

Raich JW, Potter CS (1995) Global patterns of carbon-dioxide emissions from soils. *Global Biogeochemical Cycles*, **9**, 23–36.

Reich PB, Walters MB, Ellsworth DS (1997) From tropics to tundra: global convergence in plant functioning. *Proceedings of the National Academy of Sciences of the United States of America*, **94**, 13730–13734.

Rozema J, Tosserams M, Nelissen HJM, vanHeerwaarden L, Broekman RA, Flierman N (1997) Stratospheric ozone reduction and ecosystem processes: enhanced UV-B radiation affects chemical quality and decomposition of leaves of the dune grassland species *Calamagrostis epigeios*. *Plant Ecology*, **128**, 284–294.

Schlesinger WH (1997) *Biogeochemistry: An Analysis of Global Change*. Academic Press, New York.

Swank WT, Vose JM (1997) Long-term nitrogen dynamics of Coweeta forested watersheds in the southeastern United States of America. *Global Biogeochemical Cycles*, **11**, 657–671.

Swift MJ, Heal OW, Anderson JM (1979) *Decomposition in Terrestrial Ecosystems*. Blackwell Scientific Publishing, Oxford, UK.

Trofymow JA (1998) Detrital carbon fluxes and microbial activity in successional Douglas-fir forests. *Northwest Science*, **72**, 51–53.

Trofymow JA, Moore TR, Titus B *et al*. (2002) Rates of litter decomposition over 6 years in Canadian forests: influence of litter quality and climate. *Canadian Journal of Forest Research-Revue Canadienne De Recherche Forestiere*, **32**, 789–804.

United States Environmental Protection Agency Clean Air Status and Trends Network, CASTNET (2005) Coweeta atmospheric nitrogen deposition data (COW137). http://www.epa.gov/castnet/

Virzo De Santo A, Berg B, Rutigliano FA, Alfani A, Fioretto A (1993) Factors regulating early-stage decomposition of needle litters in five different coniferous forests. *Soil Biology and Biochemistry*, **25**, 1423–1433.

Vitousek PM (1994) Beyond global warming – ecology and global change. *Ecology*, **75**, 1861–1876.

Weltzin JF, Loik ME, Schwinning S *et al*. (2003) Assessing the response of terrestrial ecosystems to potential changes in precipitation. *Bioscience*, **53**, 941–952.

Wieder RK, Lang GE (1982) A critique of the analytical methods used in examining decomposition data obtained from litter bags. *Ecology*, **63**, 1636–1642.

Appendix A Models tested for hypotheses 1–5 (H1–H5)

Table A1

Hypothesis	Model #	Model form	Δr	w_r	Converged?
H1					
	1	$M_t = M_1 \times \exp(-k_1 \times \mathrm{CDI} \times t)$	908.5	5.38E-198	Yes
	2	$M_t = M_1 \times \exp(-k_1 \times \mathrm{CDI} \times t) + M_2 \times \exp(-k_2 \times \mathrm{CDI} \times t)$	598.7	1.00E-130	Yes
	3	$M_t = M_1 \times \exp(-k_1 \times \mathrm{CDI} \times t) + M_2 \times \exp(-k_2 \times \mathrm{CDI} \times t) + M_3 \times \exp(-k_3 \times \mathrm{CDI} \times t)$	0	1	Yes
H2					
	1	$M_t = M_1 \times \exp(-k_1 \times \mathrm{CDI} \times t)$	1165.2	8.73E-254	Yes
	2	$M_t = M_1 \times \exp(-k_1 \times \mathrm{CDI} \times t) + M_2 \times \exp(-k_2 \times \mathrm{CDI} \times t)$	855.4	1.63E-186	Yes
	3	$M_t = M_1 \times \exp(-\mathrm{k}_1 \times \mathrm{CDI} \times t) + M_2 \times \exp(-k_2 \times \mathrm{CDI} \times t) + M_3 \times \exp(-\mathrm{k}_3 \times \mathrm{CDI} \times t)$	256.7	1.62E-56	Yes
	4	$M_t = M_1 \times \exp(-k_1 \times \mathrm{CDI} \times \mathrm{cell/L} \times t)$	1052.2	3.02E-229	Yes
	5	$M_t = M_1 \times \exp(-k_1 \times \mathrm{CDI} \times t) + M_2 \times \exp(-k_2 \times \mathrm{CDI} \times \mathrm{cell/L} \times t)$	99.0	2.86E-22	Yes
	6	$M_t = M_1 \times \exp(-k_1 \times \mathrm{CDI} \times t) + M_2 \times \exp(-\mathrm{k}_2 \times \mathrm{CDI} \times \mathrm{cell/L} \times t) + M_3 \times \exp(-k_3 \times \mathrm{CDI} \times t)$	11.0	0.0038	Yes
	7	$M_t = M_1 \times \exp(-k_1 \times \mathrm{CDI} \times L_c \times t)$	752.1	4.49E-164	Yes
	8	$M_t = M_1 \times \exp(-k_1 \times \mathrm{CDI} \times t) + M_2 \times \exp(-k_2 \times \mathrm{CDI} \times L_c \times t)$	230.8	7.01E-51	Yes
	9	$M_t = M_1 \times \exp(-k_1 \times \mathrm{CDI} \times t) + M_2 \times \exp(-\mathrm{k}_2 \times \mathrm{CDI} \times L_c \times t) + M_3 \times \exp(-k_3 \times \mathrm{CDI} \times t)$	16.6	0.0002	Yes
	10	$M_t = M_1 \times \exp[-k_1 \times \mathrm{CDI} \times (\exp(-b \times L_s)) \times t]$	750.2	1.15E-163	Yes
	11	$M_t = M_1 \times \exp(-k_1 \times \mathrm{CDI} \times t) + M_2 \times \exp[-k_2 \times \mathrm{CDI} \times (\exp(-b \times L_s)) \times t]$	98.9	3.08E-22	Yes
	12	$M_t = M_1 \times \exp(-k_1 \times \mathrm{CDI} \times t) + M_2 \times \exp[-k_2 \times \mathrm{CDI} \times (\exp(-b \times L_s)) \times \mathrm{t}] + M_3 \times \exp(-k_3 \times \mathrm{CDI} \times t)$	0	0.9182	Yes
	13	$M_t = M_1 \times \exp(-k_1 \times \mathrm{CDI} \times \mathrm{N/C} \times t)$	1348.9	1.1E-293	Yes
	14	$M_t = M_1 \times \exp(-k_1 \times \mathrm{CDI} \times t) + M_2 \times \exp(-k_2 \times \mathrm{CDI} \times \mathrm{N/C} \times t)$	1196.2	1.6E-260	Yes
	15	$M_t = M_1 \times \exp(-k_1 \times \mathrm{CDI} \times t) + M_2 \times \exp(-k_2 \times \mathrm{CDI} \times \mathrm{N/C} \times t) + M_3 \times \exp(-k_3 \times \mathrm{CDI} \times t)$	115.9	6.2E-26	Yes
	16	$Mt = M_1 \times \exp(-k_1 \times \mathrm{CDI} \times \mathrm{N/L} \times t)$	1103.6	2.1E-240	Yes
	17	$Mt = M_1 \times \exp(-k_1 \times \mathrm{CDI} \times t) + M_2 \times \exp(-k_2 \times \mathrm{CDI} \times \mathrm{N/L} \times t)$	453.4	3.3E-99	Yes
	18	$Mt = M_1 \times \exp(-k_1 \times \mathrm{CDI} \times t) + M_2 \times \exp(-k_2 \times \mathrm{CDI} \times \mathrm{N/L} \times t) + M_3 \times \exp(-k_3 \times \mathrm{CDI} \times t)$	29.7	3.2E-07	Yes
	19	$Mt = M_1 \times \exp[-k_2 \times \mathrm{CDI} \times (1-\mathrm{L/cell}) \times t]$	1433.5	0	Yes
	20	$Mt = M_1 \times \exp(-k_1 \times \mathrm{CDI} \times t) + M_2 \times \exp[-k_2 \times \mathrm{CDI} \times (1\text{-L/cell}) \times t]$	341.5	6.44E-75	Yes
	21	$Mt = M_1 \times \exp(-k_1 \times \mathrm{CDI} \times t) + M_2 \times \exp[-k_2 \times \mathrm{CDI} \times (1\text{-L/cell}) \times t] + M_3 \times \exp(-k_3 \times \mathrm{CDI} \times t)$	112.1	4.18E-25	Yes
	22	$Mt = M_1 \times \exp[-k_2 \times \mathrm{CDI} \times (\mathrm{L} + \mathrm{cell})/\mathrm{L} \times t]$	844.9	3.1E-184	Yes
	23	$Mt = M_1 \times \exp(-k_1 \times \mathrm{CDI} \times t) + M_2 \times \exp[-k_2 \times \mathrm{CDI} \times (\mathrm{L} + \mathrm{cell})/\mathrm{L} \times t]$	163.8	2.46E-36	Yes
	24	$Mt = M_1 \times \exp(-k_1 \times \mathrm{CDI} \times t) + M_2 \times \exp[-k_2 \times \mathrm{CDI} \times (\mathrm{L} + \mathrm{cell})/\mathrm{L} \times t] + M_3 \times \exp(-k_3 \times \mathrm{CDI} \times t)$	4.9	0.077729	Yes
H3					
	1	$Mt = M_1 \times \exp(-k_1 \times \mathrm{CDI} \times t) + M_2 \times \exp[-k_2 \times \mathrm{CDI} \times (\exp(-b \times \mathrm{L_s})) \times t] + M_3 \times \exp(-k_3 \times \mathrm{CDI} \times t)$			
		Measured chemistry	161.7	5.23E-36	Yes
		Measured chemistry and N/C modifying k_1: $M_1 \times \exp(-k_1 \times \mathrm{N/C} \times \mathrm{CDI} \times t)$	59.7	7.40E-14	Yes
		Measured chemistry and N/L modifying k_1: $M_1 \times \exp(-k_1 \times \mathrm{N/L} \times \mathrm{CDI} \times t)$	108.1	2.33E-24	Yes
		Measured chemistry and N modifying k_1: $M_1 \times \exp(-k_1 \times \mathrm{N} \times \mathrm{CDI} \times t)$	76.9	1.35E-17	Yes
		$M_2 + M_3 = [\beta_1 + \beta_2 \times (\mathrm{L/N})]$ Maximum $M_2 + M_3$ = estimated			No
		$M_2 + M_3 = [\beta_1 + \beta_2 \times (\mathrm{L/N})]$ Maximum $M_2 + M_3 = 80\%$			No
		$M_2 + M_3 = [\beta_1 + \beta_2 \times (\mathrm{L/N})]$ Maximum $M_2 + M_3 = 90\%$			No
		$M_2 + M_3 = [\beta_1 + \beta_2 \times (\mathrm{L/N})]$ Maximum $M_2 + M_3 = 95\%$			No

Continued

Table A1 *Continued*

Hypothesis	Model #	Model form	Δr	w_r	Converged?
		$M_2 + M_3 = [\beta_1 + \beta_2 \times (L/N)]$ Maximum L/N = estimated	2.0	2.50E-01	Yes
		$M_2 + M_3 = [\beta_1 + \beta_2 \times (L/N)]$ Maximum L/N = 50	24.1	4.01E-06	Yes
		$M_2 + M_3 = [\beta_1 + \beta_2 \times (L/N)]$ Maximum L/N = 60	0	6.85E-01	Yes
		$M_2 + M_3 = [15 + 1.8 \times (L/N)]$ Maximum $M_2 + M_3 = 80\%$	100.4	1.10E-22	Yes
		$M_2 + M_3 = [15 + 1.3 \times (L/N)]$ Maximum $M_2 + M_3 = 80\%$	103.2	2.69E-23	Yes
		$M_2 + M_3 = 100 - [\beta_0 + \beta_1 \times \exp(-\beta_2 \times (L/N))]$ Maximum $M_2 + M_3$ = estimated	18.3	7.27E-05	Yes
		$M_2 + M_3 = 100 - [\beta_0 + \beta_1 \times \exp(-\beta_2 \times (L/N))]$ Maximum $M_2 + M_3 = 80\%$	50.1	9.14E-12	Yes
		$M_2 + M_3 = 100 - [\beta_0 + \beta_1 \times \exp(-\beta_2 \times (L/N))]$ Maximum $M_2 + M_3 = 90\%$	28.0	5.77E-07	Yes
		$M_2 + M_3 = 100 - [\beta_0 + \beta_1 \times \exp(-\beta_2 \times (L/N))]$ Maximum $M_2 + M_3 = 95\%$	21.1	1.82E-05	Yes
		$M_2 + M_3 = 100 - [\beta_0 + \beta_1 \times \exp(-\beta_2 \times (L/N))]$ Maximum L/N = estimated	18.3	7.27E-05	Yes
		$M_2 + M_3 = 100 - [\beta_0 + \beta_1 \times \exp(-\beta_2 \times (L/N))]$ Maximum L/N = 50	32.0	7.89E-08	Yes
		$M_2 + M_3 = 100 - [\beta_0 + \beta_1 \times \exp(-\beta_2 \times (L/N))]$ Maximum L/N = 60	23.0	7.06E-06	Yes
	2	$M_t = M_1 \times \exp(-k_1 \times CDI \times t) + M_2 \times \exp[-k_2 \times CDI \times (\exp(-b \times L_{sest})) \times t] + M_3 \times \exp(-k_3 \times CDI \times t)$			
		where $L_{sest} = L/(cell + L)$ using each equation to estimate percentage cellulose			
		$M_2 + M_3 = [\beta_1 + \beta_2 \times (L/N)]$ Maximum $M_2 + M_3$ = estimated	41.3	7.55E-10	Yes
		$M_2 + M_3 = [\beta_1 + \beta_2 \times (L/N)]$ Maximum $M_2 + M_3 = 80\%$			No
		$M_2 + M_3 = [\beta_1 + \beta_2 \times (L/N)]$ Maximum $M_2 + M_3 = 90\%$			No
		$M_2 + M_3 = [\beta_1 + \beta_2 \times (L/N)]$ Maximum $M_2 + M_3 = 95\%$			No
		$M_2 + M_3 = [\beta_1 + \beta_2 \times (L/N)]$ Maximum L/N = estimated	11.7	0.002010	Yes
		$M_2 + M_3 = [\beta_1 + \beta_2 \times (L/N)]$ Maximum L/N = 50	43.7	2.27E-10	Yes
		$M_2 + M_3 = [\beta_1 + \beta_2 \times (L/N)]$ Maximum L/N = 60	9.6	0.005507	Yes
		$M_2 + M_3 = [15 + 1.8 \times (L/N)]$ Maximum $M_2 + M_3 = 80\%$	61.0	3.85E-14	Yes
		$M_2 + M_3 = [15 + 1.3 \times (L/N)]$ Maximum $M_2 + M_3 = 80\%$	40.1	1.36E-09	Yes
		$M_2 + M_3 = 100 - [\beta_0 + \beta_1 \times \exp(-\beta_2 \times (L/N))]$ Maximum $M_2 + M_3$ = estimated	25.0	2.58E-06	Yes
		$M_2 + M_3 = 100 - [\beta_0 + \beta_1 \times \exp(-\beta_2 \times (L/N))]$ Maximum $M_2 + M_3 = 80\%$	51.0	5.85E-12	Yes
		$M_2 + M_3 = 100 - [\beta_0 + \beta_1 \times \exp(-\beta_2 \times (L/N))]$ Maximum $M_2 + M_3 = 90\%$	32.4	6.32E-08	Yes
		$M_2 + M_3 = 100 - [\beta_0 + \beta_1 \times \exp(-\beta_2 \times (L/N))]$ Maximum $M_2 + M_3 = 95\%$	26.8	1.05E-06	Yes
		$M_2 + M_3 = 100 - [\beta_0 + \beta_1 \times \exp(-\beta_2 \times (L/N))]$ Maximum L/N = estimated	25.0	2.58E-06	Yes
		$M_2 + M_3 = 100 - [\beta_0 + \beta_1 \times \exp(-\beta_2 \times (L/N))]$ Maximum L/N = 50	28.5	4.47E-07	Yes
		$M_2 + M_3 = 100 - [\beta_0 + \beta_1 \times \exp(-\beta_2 \times (L/N))]$ Maximum L/N = 60	16.3	0.000199	Yes
H4 and H5					
	1	$M_t = M_{1est} \times \exp(-k_1 \times CDI \times t) + M_{2est} \times \exp[-k_2 \times CDI \times (\exp(-b \times L_{sest})) \times t] + M_3 \times \exp(-k_3 \times CDI \times t)$			
		Model tested with each CDI or climate indicator:			
		Actual evapotranspiration (AET)	764.7	0.000	Yes
		Mean annual precipitation (MAP)	812.0	0.000	Yes
		Potential evapotranspiration (PET)	1220.2	0.000	Yes
		Mean annual temperature (MAT)	3672.3	0.000	Yes
		$CDI = F_t \times F_w$			
		$F_W = [1/(1 + 30 \times \exp(-8.5 \times PPT/PET))]$			
		F_T equations			

		Linear (CDI_{linear}) = 0.198306 + T × 0.036377			No
		Exponential (CDIexp) = 0.139686 × exp(0.142064 × T)	382.8	0.000	Yes
		Llyod and Taylor (CDI_{LT}) = 0.57658 × exp[308.56 × (1/56.02−1/((273 + T)−227.13))]	0	0.986	Yes
		Arctangent (CDI_{atan}) = 11.4 + [29.7 × atan(π × 0.0309 × T−15.7)]/π	8.6	0.014	Yes
		CENTURY (CDI_{DEFAC}) = 3.439423 × exp[0.2/2.63 × (1−(45−T)$^{2.63}$/(45−35)$^{2.63}$) × (45−T)$^{0.2}$/(45−35)$^{0.2}$]	55.0	0.000	Yes
		Kirschbaum (CDI_K) = 3.909134 × exp[−3.67 + 0.204 × T × (1−0.5 × T/37)] where T stands for temperature in degrees celsius	112.7	0.000	Yes
		CDI_{atan} was normalized to the value of the equation at 30°C			
Systematic deviations					
	All litter	$M_t = M_1 \times \exp(-k_1 \times CDI_{LT} \times t) + M_2 \times \exp[-k_2 \times CDI_{LT} \times (\exp(-b \times L_s)) \times t] + M_3 \times \exp(-k_3 \times CDI_{LT} \times t)$	68.8	1.15E-15	Yes
	Litter separate	M_t = Leaf × [$M_1 \times \exp(-k_1 \times CDI_{LT} \times t) + M_2 \times \exp[-k_2 \times CDI_{LT} \times (\exp(-b \times L_s)) \times t] + M_3 \times \exp(-k_3 \times CDI_{LT} \times t)$] + Root × [$M_1 \times \exp(-k_1 \times CDI_{LT} \times t) + M_2 \times \exp[-k_2 \times CDI_{LT} \times (\exp(-b \times L_s)) \times t] + M_3 \times \exp(-k_3 \times CDI_{LT} \times t)$]	0	1	Yes
	All litter	$M_t = M_1 \times \exp(-k_1 \times CDI_{LT} \times t) + M_2 \times \exp[-k_2 \times CDI_{LT} \times (\exp(-b \times L_s)) \times t] + M_3 \times \exp(-k_3 \times CDI_{LT} \times t)$	209.7	0.0	Yes
	Wetlands separate	M_t = Terrestrial × [$M_1 \times \exp(-k_1 \times CDI_{LT} \times t) + M_2 \times \exp[-k_2 \times CDI_{LT} \times (\exp(-b \times L_s)) \times t] + M_3 \times \exp(-k_3 \times CDI_{LT} \times t)$] + Wetland × [$M_1 \times \exp(-k_1 \times CDI_{LT} \times t) + M_2 \times \exp[-k_2 \times CDI_{LT} \times (\exp(-b \times L_s)) \times t] + M_3 \times \exp(-k_3 \times CDI_{LT} \times t)$]	200.3	3.26E-44	Yes
	Wetland roots separate	M_t = Wetland root × [$M_1 \times \exp(-k_1 \times CDI_{LT} \times t) + M_2 \times \exp[-k_2 \times CDI_{LT} \times (\exp(-b \times L_s)) \times t] + M_3 \times \exp(-k_3 \times CDI_{LT} \times t)$] + all other × [$M_1 \times \exp(-k_1 \times CDI_{LT} \times t) + M_2 \times \exp[-k_2 \times CDI_{LT} \times (\exp(-b \times L_s)) \times t] + M_3 \times \exp(-k_3 \times CDI_{LT} \times t)$]	0	1	Yes
	All litter	$M_t = M_1 \times \exp(-k_1 \times CDI_{LT} \times t) + M_2 \times \exp[-k_2 \times CDI_{LT} \times (\exp(-b \times L_s)) \times t] + M_3 \times \exp(-k_3 \times CDI_{LT} \times t)$	0	1	Yes
	Arctic roots separate	M_t = Arctic root × [$M_1 \times \exp(-k_1 \times CDI_{LT} \times t) + M_2 \times \exp[-k_2 \times CDI_{LT} \times (\exp(-b \times L_s)) \times t] + M_3 \times \exp(-k_3 \times CDI_{LT} \times t)$] + all other × [$M_1 \times \exp(-k_1 \times CDI_{LT} \times t) + M_2 \times \exp[-k_2 \times CDI_{LT} \times (\exp(-b \times L_s)) \times t] + M_3 \times \exp(-k_3 \times CDI_{LT} \times t)$]	210	2.88E-46	Yes
	All litter	$M_t = M_1 \times \exp(-k_1 \times CDI_{LT} \times t) + M_2 \times \exp(-k_2 \times CDI_{LT} \times (\exp(-b \times L_s)) \times t) + M_3 \times \exp(-k_3 \times CDI_{LT} \times t)$	74.0	9.9E-22	Yes
	Temperate and Tropical site N multiplier	$\text{N Multiplier}\,(E_N^k) = \begin{cases} 5.0 & \text{if L/cell}^k \le 0.2 \\ 2.0 + (0.4\text{L/cell}^k) \times 15 & \text{if L/cell}^k > 0.2 \text{ and } \le 0.4 \\ 2.0 & \text{if L/cell}^k > 0.4 \end{cases}$	0	1	na
		$L/N_{initial}^k = L^k/(N^k \times E_N^k)$			

k, litter type, $L/N_{initial}^k$, initial lignin/nitrogen ratio of litter type k, L^k, initial lignin concentration of litter type k, N^k, initial nitrogen concentration of litter type k, $L/cell^k$, initial lignin/cellulose of litter type k.
na, no parameters were fit.

Table of abbreviations

L	Initial lignin content (%)
Cell	Initial cellulose content (%)
C	Initial carbon content (%)
N	Initial nitrogen content (%)
M_t	Mass remaining at time, t
M_p	Initial mass of each pool, p
M_{pest}	Initial mass of each pool, p, estimated using initial pool equation from H3
L_s	L/(L + cell)
L_c	$-3 \times L_s$
CDI_j	Climate decomposition index for site, j
CDI_{LT}	CDI with Lloyd and Taylor temperature function (Lloyd & Taylor, 1994)
CDI_{atan}	CDI with arctangent temperature function (Del Grosso *et al*., 2005)
CDI_K	CDI with Kirschbaum *et al*. (1995) temperature function
CDI_{exp}	CDI with exponential temperature function
CDI_{Linear}	CDI with linear temperature function
CDI_{DEFAC}	CDI with CENTURY's DEFAC temperature function (Parton *et al*., 1994)

Appendix B Parameter estimate correlation matrices for best models from hypotheses 1–5 (H1–H5)

Table B1

	Correlation coefficients (r)					
	k_1	k_2	k_3	b	a	z
H1						
k_1	1	−0.7867				
k_2	−0.7867	1				
k_3						
H2						
k_1	1	0.1068	0.3751	0.3997		
k_2	0.1068	1	0.4281	0.8576		
k_3	0.3751	0.4281	1	0.7424		
b	0.3997	0.8576	0.7424	1		
H3 and H5						
k_1	1	0.3323	−0.2761	−0.3190	−0.6947	0.4738
k_2	0.3323	1	−0.1893	0.4651	−0.4839	0.1790
k_3	−0.2761	−0.1893	1	0.5351	0.2248	−0.4225
b	−0.3190	0.4651	0.5351	1	0.0490	−0.5668
a	−0.6947	−0.4839	0.2248	0.0490	1	0.0349
z	0.4738	0.1790	−0.4225	−0.5668	0.0349	1
H4						
k_1	1	0.1871	−0.2123	−0.3452	−0.6814	0.3488
k_2	0.1871	1	−0.0333	0.6298	−0.3987	−0.0667
k_3	−0.2123	−0.0333	1	0.4544	0.1879	−0.2639
b	−0.3452	0.6298	0.4544	1	0.0864	−0.5229
a	−0.6814	−0.3987	0.1879	0.0864	1	0.2130
z	0.3488	−0.0667	−0.2639	−0.5229	0.2130	1